January 2019

# Low-Density Static Granular Media Filter Bed Turbidity Removal Model

Matthew Louque
mlouqu4@lsu.edu

# Low-Density Static Granular Media Filter Bed Turbidity Removal Model

A Thesis

Submitted to the Graduate Faculty of the
Louisiana State University and
Agricultural and Mechanical College
in partial fulfillment of the
requirements for the degree of
Masters of Science in Civil Engineering

In

The Department of Civil & Environmental Engineering

By
Matthew Tyler Louque
B.S., Louisiana State University 2016
May 2019

# Acknowledgements

This thesis was only possible with the support and assistance of several individuals. I would like to acknowledge those who have been a part of this journey.

I owe my deepest gratitude to Dr. Ronald Malone, my mentor, head advisor, and Emeritus Professor at Louisiana State University Department of Civil and Environmental Engineering. Dr. Malone's office and home have been open to me throughout the past five years. He has challenged me to take on new and difficult tasks while continuously offering his expertise and wisdom. I will be forever grateful for his influence and guidance. And to his wife and my mother away from home, Mrs. Sandra Malone, I offer my thanks for opening her heart and home and providing a listening ear to me.

I would also like to thank Dr. Celalettin Ozdemir and Dr. Chandra Theegala for being on my thesis committee and giving me direction throughout this process. I could not have completed my research project without your support and input.

I must also thank my mother, Gail Louque, for taking on the role of mother and father in my life and always providing reassurance that I am capable of reaching my highest goals. Without her support, I would not have had the ambition to move out of our small town to pursue a career in engineering. I am grateful to my older sister, Brandi Chatelain, for standing by my side throughout my entire life, and providing advice when needed.

Finally, I must express my gratitude to my sister and brother-in-law, Samantha and Kendall Lemelle. Their home has always been open to me, and they've supported me both emotionally and financially. Since the day I was born, Samantha has taken on the role of being my guardian. She has given me advice – even when I don't want to hear it – and has always truly wanted what's best for me.

This work is supported by USDA-SBRI Aquaculture Grant no. 11336472 / project accession no.1000518 from the USDA National Institute of Food and Agriculture.

# TABLE OF CONTENTS

# List of Tables

# List of Figures

# Abstract

The scattering of light within a fluid, referred to as its turbidity, was investigated against the presence of suspended solids. A linear regression analysis was conduced against turbidity and the total count, combined surface area, and combined volume of the suspended particles for various surface water sources (lakes, rivers, indoor aquaculture systems). It was found that the total combined surface area of suspended particles had the best linear correlation to turbidity, with an adjusted $R^2$ of 81.79%. This correlation was integrated with a current theoretical model for predicting solids removal across a granular bed to yield an Integrated Turbidity Removal Model. This model was then calibrated against three different media types at three different flux rates, and proved to be a reasonably accurate at predicting the effectiveness of the granular bed on removing turbidity. A sensitivity analysis was conducted using the newly calibrated Integrated Turbidity Removal Model and it found that the variables that impact the effectiveness of the bed to remove turbidity the most are the particle density, filtration rate (flux rate), and media size.

# Chapter 1. Introduction

## 1.1. Introduction

The research conducted for this study was initiated off of an USDA SBIR Research Grant (grant no. 11336472; project accession no. 1000518) awarded to Aquaculture Systems Technologies (AST) to apply direct filtration methods, using floating media and flocculent aids, for fine suspended solids and phosphorus removal. This research grant was addressed specifically to marine systems. In this context, clarity of the effluent waters is the primary concern of marine farmers. During preliminary tests, it was noticed that a majority of the solids could be removed with this filtration technique; however, the effluent waters still remained slightly turbid. To address this turbidity issue, further investigation was conducted to determine the correlation between the suspended particles and turbidity to design an effective granular filter to reach a given turbidity value.

The specific objectives for this effort are as follows: (1) Determining a correlation between suspended particles and turbidity. (2) Identifying a theoretical model to predict solids removal across a granular bed. (3) Combining the correlation between suspended particles and turbidity, to the theoretical solids-removal model to form a cohesive integrated model capable of predicting turbidity removal across a granular bed. (4) Calibration / verification of the integrated model.

## 1.2. Suspended Solids

Solids management is a fundamental element of maintaining water quality, be it in a marine or wastewater setting. The presence of solids is a good indicator for microbial life within a given system, since the solids provide both a food source and the required surface area for their growth. Solids are typically measured as total suspended solids (TSS); however, it can also be measured indirectly as turbidity. There are many ways to remove these solids from water, but one of the most common and oldest methods of removal is through the use of granular filtration.

## 1.3. Turbidity

Turbidity is a measurement of scattered light within a fluid. The higher a fluid's turbidity, the more difficult it is for light to transmit through it thus making it appear cloudy or even opaque to the observer. To the general public, turbidity of a system is one of the most important parameters to minimize since generally, the physical appearance of the water is the number one indicator on judging the quality of the water.

Common measuring practices involve directing a light beam through a fluid and measuring the intensity of the light scattered 90 degrees, relative to the incident light. All particles do not scatter light equally.

## 1.4. Methods of Solids Capturing

There are several ways of removing solids from a given fluid, including but not limited to: sedimentation, micro-screens, and granular filtration such as sand or floating bead filters. A more thorough description of each method will be explained in this section.

### 1.4.1. Sedimentation

Sedimentation utilizes gravity as the main driving force to remove solids. Solids denser than the containing fluid will settle without external energy input for their removal. The physical properties of sedimentation are described in Lawson (1994), Weber (1972), and Wheaton (1977). While sedimentation is great at removing the bulk of suspended solids (SS), it alone is not sufficient enough at removing all SS. This inefficiency is outlined in Chessness et al. (1975) and Chiang and Lee (1986). This is due to micro-particles, typically < 100 microns, having a minimal or even non-existent settling velocity based on the Stokes Law. According to Cripps (1993), the majority of particles constituting TSS are below 30 microns in diameter; which is also reinforced in Chen et al. (1993) where he claims 95% of suspended particles, by count in a recirculating aquaculture system (RAS) system, are under 20 microns in diameter.

### 1.4.2. Micro-screen

Microscreens utilize a fabricated mesh screen to intercept and filter out suspended solids. Micro-screens are especially effective for high solids concentration flows and there are many different configurations of microscreen filters, such as: static screening, rotating microscreens, and drum filters (Makinen et al., 1988; Tchobanoglous and Burton, 1991; Cripps and Kelly, 1996; Wheaton, 1977; Huguenin and Colt, 1989; Twarowska et al., 1997). Pore sizes of 60 – 200 microns are common, since there is little advantage to using pore sizes smaller than 60 microns (Cripps and Bergheim, 2000). The limitations on this technology include: high water loss (10 – 20 liters of sludge water per cubic meter of tank effluent) for standard backwashing (Bergheim et al., 1993a), and low solids removal rates

at low solids concentration. Low-concentration aquaculture solids that have no agglomeration of particles are prone to have technical issues with solids removal when using microscreens (Cripps and Bergheim 2000) such as clogging.

### 1.4.3. Sand Filtration

Sand filtration uses a static bed of fine granular media (sand) to intercept and remove solids from a fluid. It is one of the most common methods of removing TSS from water or wastewater. The efficiency of this type of filtration is well documented, with TSS removal rates averaging around 83.33-98.35% for wastewaters (Owen and Bobb, 1994; Louden et al., 1985; Piluk and Peters, 1994; Roy and Dube, 1994). TSS removal rates of 100% have been achieved such as the experiment conducted in Healy et al. (2007) where a stratified sand filter was used on dairy wastewater with sand/gravel. The limitations of this technology are the high-energy demand needed to flow through such a fine media, high water loss from backwashing, and the media is prone to biofouling. The high water loss also makes this method of filtration unable to be used in RAS applications.

### 1.4.4. Floating Bead Filtration

Floating bead filters uses a static bed of low-density (specific gravity (SG) = 0.92 – 0.94) floating media, typically polypropylene, to intercept and remove solids from a fluid. The media used in these filters were designed to overcome the limitations of fine granular media (sand, gravel, etc.). In comparison, the relative size of the floating media is much larger than the size of sand. This increases pore space when the media is shaped (see EN media), allowing a lower energy cost for filtration and minimal water loss when

backwashing. Another benefit of larger, constructed media is that it can be designed to increase surface area. This allows floating bead filters to have enhanced bio-filtration capabilities without biofouling issues when treating high organic loadings (Malone and Beecher, 2000).

In terms of water clarity, Visvanathan et al. (1996) determined duel-media, composed of Polypropylene and Polystyrene (diameter of 2.57 mm and 1.54 mm respectively), could remove 2 – 5 times more turbidity per unit head loss, compared to standard sand filtration ($d_{10}$ = 1 mm). However, the limitation on floating bead filtration is the low removal rates for particles < 30 microns. The study of Malone and Gudipati (2007) states, "Removal efficiencies decline from nearly 100% in the 30-50 micron size range".

## 1.5. Methods of Predicting Solids Removal in Granular Bed

Determining filtration efficiency, for removing solids, is based off of the combined removal efficiency from three solids transport mechanisms (interception, sedimentation, and diffusion). Interception is when a suspended particle comes into contact with the filter media due to its own size, sedimentation occurs when the suspended particle has a higher density than the water and has its trajectory altered due to the influence of gravitational forces, and diffusion occurs when particles (predominately < 1 micron in diameter) are subjected to the random bombardment of other molecules resulting in Brownian Motion. Yao et al. (1971) published a heavily cited (1600+) paper combining these transport mechanisms and developing a model to predict filtration efficiency from parameters such as: filtration rate, bed depth, media porosity, media size, particle size, particle density, attachment efficiency, water density, and temperature.

In Yao et al. (1971), he denoted the strong correlation between coagulation and solids removal in a granular bed as an analogous process. He states that the removal of suspended particles are the same two steps for filtration and coagulation: (1) transporting the particle to the solid-liquid interface, (2) attachment of those particles to the media surface. For coagulation, transport models are primarily derived from Smoluckowski (1917), while current water filtration models are developed from air filtration models (Friedlander, 1958; Spelman and Goren, 1970; Cookson, 1970). All these models predict that suspended particles larger than about 1 micron in diameter are primarily removed through settling (gravitational forces) and interception whereas particles below 1 micron are primarily removed through diffusion. A particle with a diameter of 1 micron is also universally agreed upon as the size of lowest removal efficiency; whereby increasing its diameter increases or decreases the efficiency. This is due to Brownian motion having its effects increased as particles get smaller than 1 micron and gravitational forces having its effect increased as particles get larger than 1 micron.

# Chapter 2. Development of Turbidity Model

## 2.1. Introduction

Solids management is a fundamental element of maintaining water quality. The presence of suspended solids (SS) can be a good indicator of pathogens, viruses, algae, and bacterial flocs being present in influent waters. This is because suspended solids can essentially be regarded as a food source for microbial life, however microbial life can also live on dissolved chemicals. It can also be directly correlated with water clarity as well as the presence of organics, which is often referred to as biological oxygen demand (BOD).

The presence of suspended solids is typically measured as total suspended solids (TSS); however, it can also be measured indirectly as turbidity, which is a measurement of light scattered within a fluid. The degree to which light is scattered is dependent on the suspended particles within the fluid to facilitate that interaction. Therefore, turbidity can be a useful parameter to monitor, since it can be correlated to the presence of suspended solids and the physical appearance of the water.

The overall objective of this study is to develop an optimal method of removing turbidity. As an initial step, a theoretical analysis of the solids transport and removal mechanisms that occur during granular filtration are evaluated. The aim of this chapter is to determine a correlation between suspended particle size distributions and their conjugate turbidity measurements. Once this is evaluated and a correlation is established, the long-term goal

is then to integrate this data with current models for predicting solids removal efficiency in a granular bed to be able to predict turbidity removal. Using this integrated model, granular filters could then be designed to meet specific turbidity requirements.

## 2.2. Background

Suspended solids (SS) are particulates with varying densities and shapes that remain in suspension in a fluid medium (clays, algae, etc.). The presence of SS can be an indicator of poor water quality since SS provide additional surface area for microorganisms (pathogens, viruses, etc.) to proliferate. They also scatter light, which can cause the fluid to appear cloudy or even completely opaque.

The measure of scattered light or opacity of a fluid is referred to as its turbidity. Turbidimeters base their measurements on the intensity of light scattered 90 degrees with respect to the incident light. Turbidity is measured in several different units, however, for this study, turbidity was measured in Nephelometric Turbidity Units (NTU) where 0 NTU reflects crystal clear water and readings of 1000+ NTU reflects completely opaque water.

The intensity of scattered light in relation to SS within a fluid is directly dependent on the size of the particle relative to the wavelength of the incident light (Hach, 2018). In the same study it is found that spherical particles, $1/10^{th}$ of the size of the incident light wavelength, essentially act as a light source themselves; since these particles scatter light symmetrically in all directions. Particles sized larger starts propagating the scattered light

more forward. The shape of the particles also affects the intensity of scattered light, where spherical particles scatter light more forward / backward in comparison to rod / coiled shaped particles (Hach, 2018).

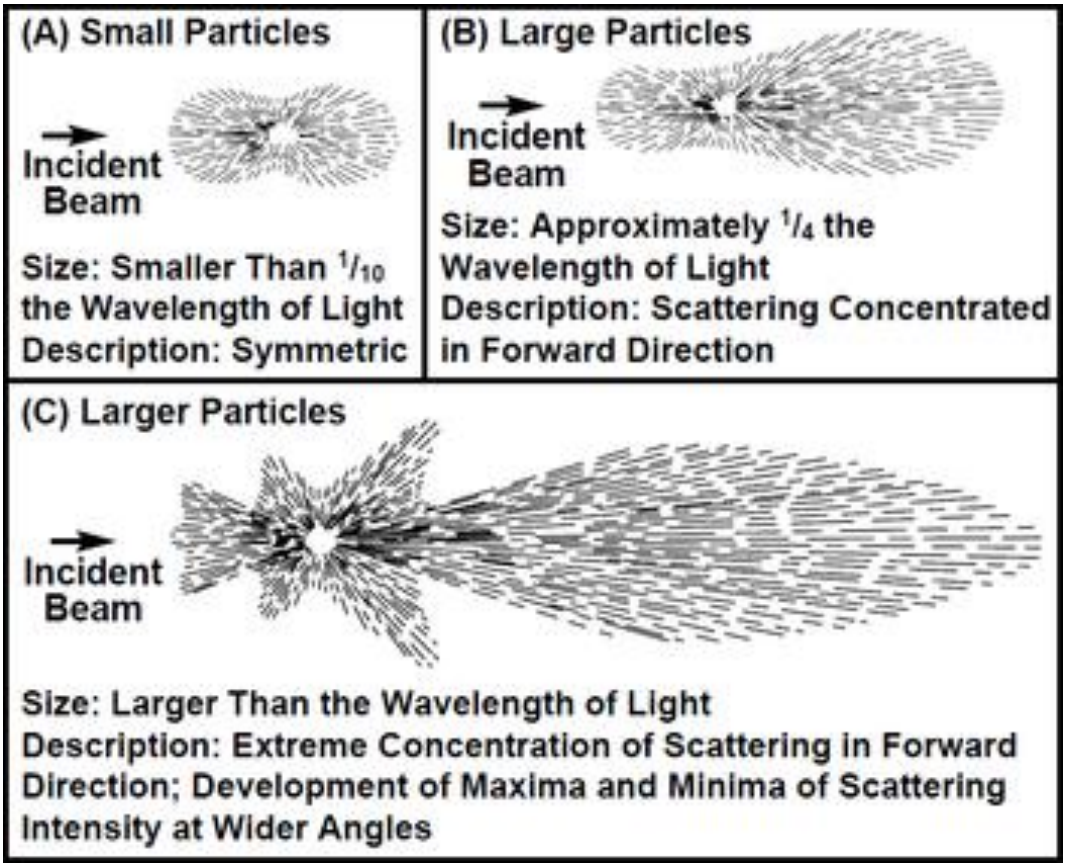

Figure 1. Hach Light Scattering vs. Particle Size Relation (Hach, 2018)

The effectiveness of TSS removal mechanisms differs with the size of the particle. For example, clarifiers are known for their ability to remove large percentages of TSS, being highly effective at removing particles >100 microns. However, if the intensity of scattered light increases, as particles get smaller, a high TSS removal rate might not necessarily correlate equally with the removal of turbidity.

Granular filtration, such as sand or bead filters, is more effective for fine solids (<100 microns) removal. The effectiveness of these types of filters is heavily dependent on their design and they impact different particle sizes differently. Different particle sizes also affect turbidity differently, and knowing the relationship between particle size and turbidity could be crucial for designing an effective granular filter for removing turbidity.

Mechanisms of solids removal during granular filtration can be essentially described by three transport mechanisms: interception, sedimentation, and diffusion. Interception occurs when the radius of the particle is larger than the distance between the streamline and the capturing media, causing the particle to come into contact with the media, where it has a chance of sticking to its surface and become effectively removed. Sedimentation occurs when the density of the particle is greater than the surrounding fluid, causing its trajectory to be altered by the streamline, allowing it to come into contact with the capturing media. Diffusion occurs for very small particles (< 1 micron) where the random bombardment of other molecules dominate their motion, allowing these sized particles to take alternate routes different from the streamline.

For suspended particles smaller than 1 micron in diameter, diffusion is the principal transport mechanism of removal. Particles sized above 1 micron have sedimentation and interception as the primary mechanisms of removal, however, according to Yao et al. (1971), sedimentation is always the principal mechanism of removal (Figure 2). Calculating the removal efficiency of a granular bed, which is dependent on these

mechanisms of solids transport, can point one in the right direction for designing an optimal filter.

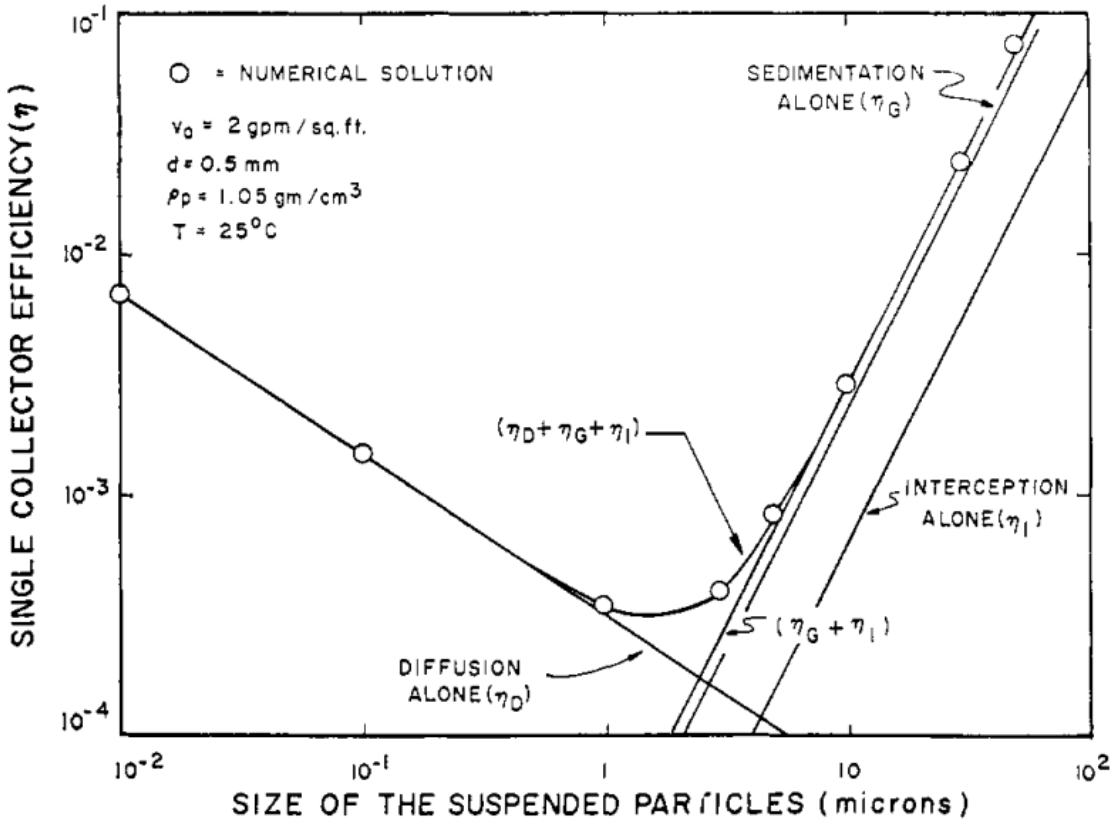


Figure 2. Yao's Collector Efficiency for Various Transport Mechanisms. The collector efficiency of each transport mechanism ($n_D$ = Diffusion, $n_G$ = Sedimentation, $n_I$ = Interception). Credit to Yao et al. (1971)

## 2.3. Materials / Methods

### 2.3.1. Overview

Since particle size impacts the nature of light scattering, there should be a correlation between the distribution of particle sizes and turbidity. According to Hach, smaller particles scatter light more. Therefore, it would be expected that water sources with a

larger amount of finer particles would yield a much higher turbidity. However, their study looked at the effect of a single particle on light scattering. In this study, the correlation between the cumulative effects of light scattering from multiple particles will be analyzed.

To analyze the correlation between particle size distributions and their conjugate turbidity measurements, a series of samples were taken from various lakes and rivers around Baton Rouge, Louisiana. It was decided that the experiment would focus on natural waters since different types of waters (such as wastewaters) could have constituents that could skew results. Samples were collected from 10 sample sites during the fall of 2017 and fall of 2018 and stored in the Aquaculture Systems Technology's (AST) laboratory at room temperature. All samples were measured within 12 hours of collection. After the data was collected and compiled [Appendix C: Raw Data], it was analyzed in Statistical Analysis System (SAS) using a multi-linear regression model (n = 10).

### 2.3.2. Location of Sample Sites

Figure 3a and 3b depicts a satellite image overview of the area with sample sites (10) marked with a golden star. Due to scaling, two of the marked sample sites will account for two separate sample sites instead of one. Names and general descriptions of the water source are included in Table 1.


Figure 3a. Sample Site Locations

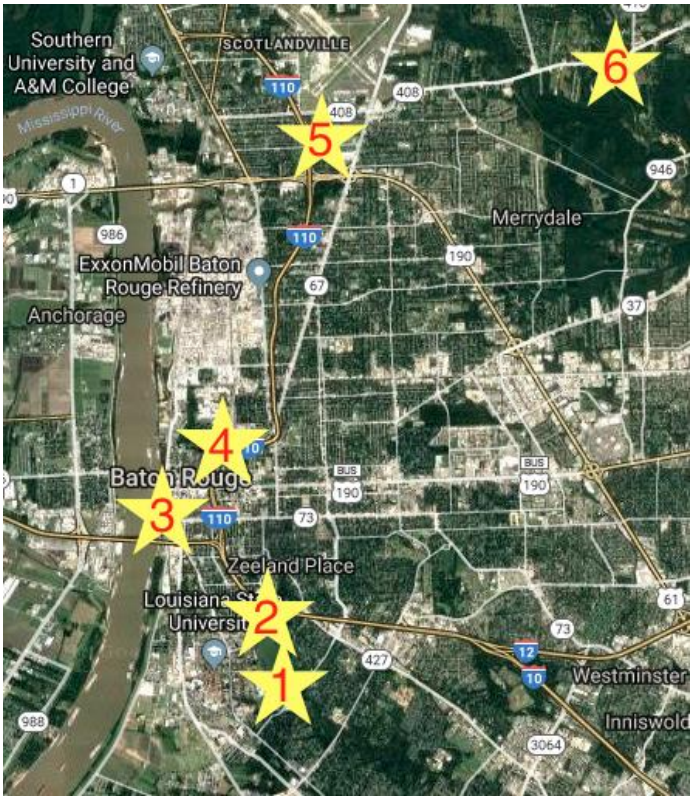


Figure 3b. Sample Site Locations

Table 1. List of Lakes / Rivers Sampled

| Name of Lake | Description |
|---|---|
| 1. University Lake and Bayou Duplanier | Light green water; light brown water |
| 2. City Park Lake | Fairly clear water |
| 3. Mississippi River (right side) | Brown water |
| 4. Capitol Lake (north and south side) | Fairly clear water |
| 5. Monte Sano Bayou | Fairly clear water |
| 6. Comite River | Fairly clear water |
| 7. Bayou Plaquemine | Fairly clear water |
| 8. Mississippi River (left side) | Brown water |

### 2.3.3. Sampling Procedures

Two liters were taken from each sample site to analyze in the laboratory. Samples were taken during noon hours (12pm – 3pm CST) in the late spring, early summer of 2018. Due to the measuring limitation of the particle size analyzer (ChemTrac Pc 3400) used, where particles greater than 100 microns are measured as ">100"; all samples were first run through a 100-micron screen to minimize errors from the presence of particles outside the scope of precise measuring. A peristaltic pump was used to gently flow the samples through the particle size analyzer to minimize the amount of particles being broken up due to the pump. Once samples were flowed through the analyzer, they were immediately flowed into a 15 mL testing vial to be analyzed by a Turbidimeter (2100Q Portable Turbidimeter). [Appendix B – Experimental Setup]

## 2.4. Statistical Analysis

Results from the particle size analyzer and their respective turbidity measurements were compiled and analyzed to determine if any correlations between the two measurements

could be formed [Appendix D – Graphical Illustrations of Statistical Regression Analysis]. Particle size distributions were translated into three variables (total count, total surface area, and total volume of particles) to be correlated to turbidity.

When looking at the correlation between the total surface area of the suspended particles (assuming they are perfectly spherical) and their respective turbidity, there was a strong linear correlation ($R^2$ = 83.81%, Adjusted-$R^2$ = 81.79%) (Appendix D – Figure 2d). This correlation is verified from the statistical analysis from SAS, where it is concluded that 81.79% of the turbidity readings could be explained by the total surface area of the suspended particles.

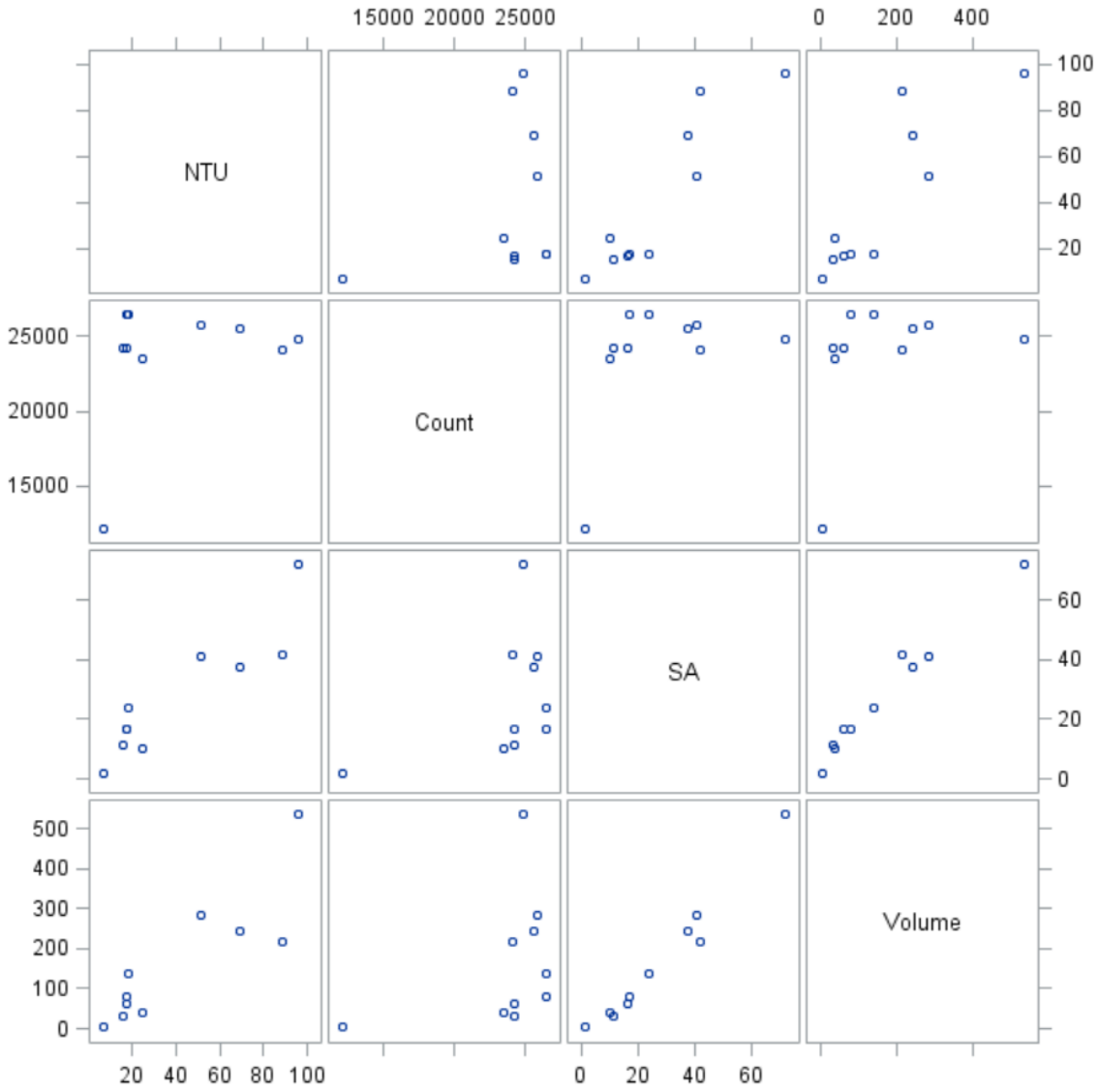

Figure 4. Regression Analysis Matrix for NTU, Count, Surface Area, & Volume

From the matrix shown in Figure 4, variables in the column are represented on the x-axis, whereas variables in the row are represented on the y-axis. Count is represented by total count of all particles sized 0 – 100 microns, surface area is represented by million-micron$^2$, and volume is represented by million-micron$^3$. The matrix shows a linear correlation between surface area and NTU as well as a looser linear correlation between volume and NTU. There is also a very strong linear correlation between surface area and volume.

Taking this linear correlation between the total surface area of all suspended particles and expected turbidity, a particular particle's contribution to turbidity can essentially be derived by taking the ratio of a specific particle's surface area over the total surface area for any given turbidity measurement.

## 2.5. Verification of Results

The linear correlation found was compared with data collected from Ms. Lisa Weaver, EI, who is a researcher at Aquaculture Systems Technology (AST) where she was researching three separate growout methods (Biofloc, Hybrid Biofloc, and PolyGeyser Fixed-Film) for intensively stocked shrimp systems. Methods of measuring were primarily similar to methods used on the lake samples; however, turbidity measurements were taken directly from the shrimp tanks rather than from the outflow from the particle size analyzer. Figure 4 below shows how Weaver's data compared.

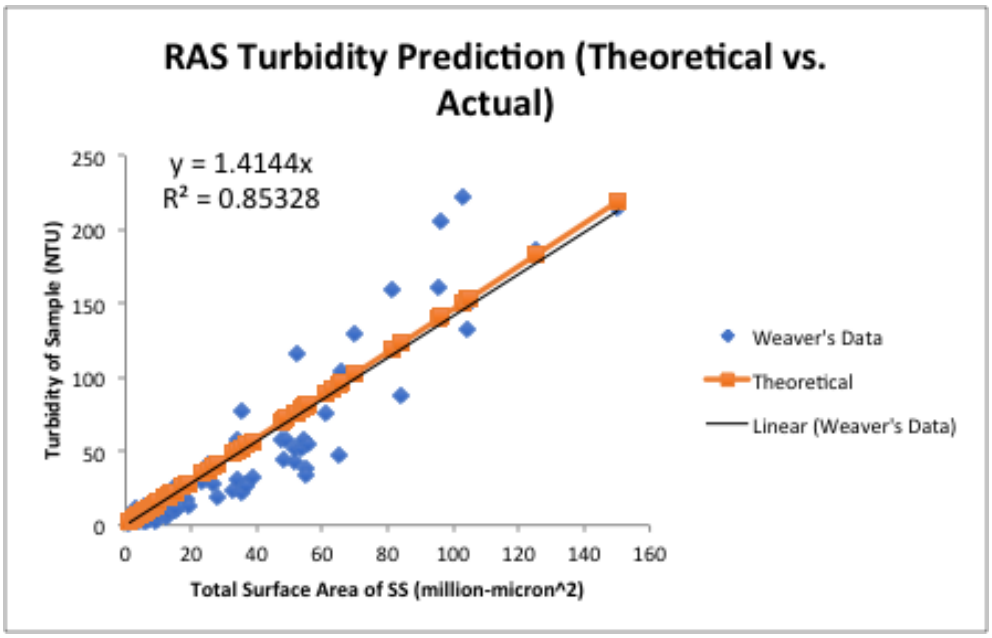


Figure 5. Verification of Turbidity Data with External Data Set. Weaver's data plotted with a linear trend line ($R^2$ = 85.33%) along with the turbidity / surface area relationship derived from the SAS analysis of the 10 sample sites.

From Figure 5, comparing the RAS data collected by Weaver (Weaver et al. 2018) to the data collected from the lakes, both data sets have similar linear trends between total surface area and turbidity ($R^2$ values between 81-85%) with slopes of 1.41 and 1.45 respectively.

## 2.6. Discussion

The turbidity model works because for light to be scattered, within a fluid, it requires a surface to reflect off of. When the amount of surface area available for the light to interact with increases, the amount of light that scatters also increases. This can be inferred from the linear projection of the NTU vs. Turbidity model, where a fairly linear relationship within the turbidity range analyzed is observed under this study.

The results gathered from the lake samples along with Weaver's RAS data shows that there is a linear correlation between total surface area of suspended particles and expected turbidity. This correlation in itself can be beneficial since any given particles surface area, as a ratio of the total measured surface area, can essentially be defined as a particles % contribution to that turbidity measurement. This allows for easy identification of problematic particle size ranges, and also serves as a useful tool for understanding the limitations of turbidity removal with technologies that have well defined removal ranges for particulates.

Typically, for this type of analysis, a power function would be used to curve fit the data since it offers two independent variables as opposed to one variable from a linear function. However, for the turbidity range chosen, a linear function intercepted at 0 provides a better fit. This is probably due to the turbidity range being so low (0 – 100). Data trends represented by power functions can essentially be broken into three separate phases: linear, transitional, and linear; the beginning and end of a data set following a power relationship are fairly linear. Since the turbidity range is so low, the data analyzed during this study would most likely fall under the first phase if the data set truly followed a power function. However, since the data set for this study was limited to a low turbidity range, it cannot be confidently asserted that the data truly follows a different function without additional data to prove it.

Knowing how surface areas of suspended particles can relate to expected turbidity values could prove to be useful when used in conjunction with current theoretical models for

filtration efficiency. Current models, such as the one derived in Yao et al. (1971), uses filtration parameters (flux rate, bed depth, media size, etc.) to estimate the removal rate for any given particle size. Combining the relation between particle size and their expected contribution to turbidity would yield a filtration model capable of predicting turbidity removal, allowing for a useful tool for designing a granular filter based off of turbidity requirements.

Application of this model allows for the assumption of a particles % contribution to turbidity (with respect to surface area) to be valid. Meaning, if a particular particle's surface area contributes 50% of the total surface area of all suspended particles, it can be assumed that that particle also contributes to 50% of the total turbidity. Removal of that particle would therefore yield a 50% reduction in turbidity. Combining this assumption with current models for solids removal could provide a model capable of predicting turbidity removal.

## 2.7. Conclusion

In conclusion, a strong linear correlation between the total surface area of all suspended solids and turbidity is observed. This shows that the degree of light scattered when passing through a fluid medium is dependent on the available surface area of the suspended particles within that medium; meaning, turbidity can be best explained by particle size distribution through the computation of their cumulative surface area. There were no apparent relations between total counts of particles or total volume of particles to turbidity. [Appendix D - Graphical Illustrations of Statistical Regression Analysis]

# Chapter 3. Development of Integrated Turbidity Removal Model

## 3.1. Introduction

Granular filtration is the method of removing particulates from source water using a bed of media to act as the interceptors. This process has been implemented by man for water treatment as early as 200 B.C according to both Sanskrit medical lore and Egyptian inscriptions (Baker, 1949). In addition, to this date, there are few treatments applications today that do not implement this method of solids removal.

Granular filtration is a versatile treatment method, allowing effective treatment for any type of fluid, be it air or water. Typically, granular filtration is set up with a static media bed, but some applications call for a dynamic bed. The type of media housed in these filters can also vary by type. Generally granular filters are filled with either sand or floating media, which are applied with typically a uniform size distribution but can also be applied with a stratified size distribution.

For the general public, the physical appearance or clarity of the water, is the biggest indicator of poor water quality. In scientific terms, clarity refers to the degree at which light is scattered within the fluid, a term measured as turbidity. Turbidity is commonly measured in Nephelometric Turbidity Units (NTU) where values of 5 NTU and less are generally invisible to the human eye. Turbidity is also a parameter regulated by the World Health Organization (WHO) and the Environmental Protection Agency (EPA) for human consumption. WHO states that in order to achieve effective disinfection requires a

minimum of 5 NTU, ideally 1 NTU (WHO, 2018). EPA mandates that effluents from conventional or direct filtration systems shall not exceed 1 NTU and shall read < 0.3 NTU 95% of the time (EPA, 2018). In the United States, common state limits require measurements not exceeding 5 NTU.

Effectiveness of a granular bed on removing solids has been extensively analyzed by academics, with theoretical models of their efficiency being well established. Combining the already established models for predicting particle size removal with the newly correlated data on turbidity and particle size can yield a theoretical model capable of predicting the effectiveness of granular beds on removing turbidity. This chapter aims to outline the development of this integrated model.

## 3.2. Background

Sand filtration uses a static bed of fine granular media (sand) to intercept and remove solids from a fluid. It is one of the most common methods of removing TSS from water or wastewater. The efficiency of this type of filtration is well documented, with total suspended solids (TSS) removal rates averaging around 83.33-98.35% (Owen and Bobb, 1994; Louden et al., 1985; Piluk and Peters, 1994; Roy and Dube, 1994). TSS removal rates of 100% have been achieved; Healy et al. (2007) used a stratified sand filter with sand/gravel. The limitations of this technology are the high-energy demand needed to flow through such a fine media, high water loss from backwashing, and the media is prone to biofouling. The high water loss also makes this method of filtration unable to be used in RAS applications.

Floating bead filters use a static bed of low-density (SG = 0.92 – 0.94) floating media, typically polyethylene, to intercept and remove solids from a fluid. The media used in these filters were designed to overcome the limitations of fine granular media (sand, gravel, etc.). In comparison, the relative size of the floating media is much larger than the size of sand. The benefit of larger, constructed media is that it can be shaped to increase surface area. This allows floating bead filters to have enhanced bio-filtration capabilities without biofouling issues when treating high organic loadings (Malone and Beecher, 2000). In terms of water clarity, Visvanathan et al. (1996) determined duel-media, composed of polypropylene and polystyrene (diameter of 2.57 mm and 1.54 mm respectively), could remove 2 – 5 times more turbidity per unit head loss, compared to standard sand filtration ($d_{10}$ = 1 mm). However, the limitation on bead filtration is the low removal rates for particles < 30 microns. "Removal efficiencies decline from nearly 100% in the 30-50 micron size range" (Malone and Gudipati 2007).

Determining filtration efficiency for removing solids is essentially the combined removal efficiency from three transport mechanisms (interception, sedimentation, and diffusion). Interception occurs when a suspended particle comes into contact with filter media due to its own size, sedimentation occurs when the suspended particle has a higher density than the water and has its trajectory altered due to the influence of gravitational forces, and diffusion occurs when particles (sized < 1 micron in diameter) are subjected to the random bombardment of other molecules resulting in Brownian motion. Yao et al. published a heavily cited (1600+) paper in 1971 combining these transport mechanisms

and developing a model to predict filtration efficiency from parameters such as: filtration rate, bed depth, media porosity, media size, particle size, particle density, attachment efficiency, water density, and temperature.

Yao et al. (1971) denotes the strong correlation between coagulation and solids removal in a filter as being an analogous process. He states the removal of suspended particles are the same two steps for filtration and coagulation: (1) transporting the particle to the solid-liquid interface, (2) attachment of those particles to the media surface. For coagulation, transport models are primarily derived from Smoluckowski (1917), and current water filtration models are developed from air filtration models (Friedlander, 1958; Spielman and Goren, 1970; Cookson, 1970) All these models predict that suspended particles larger than about 1 micron are primarily removed through settling and interception whereas particles below 1 micron are primarily removed through diffusion. A particle with a diameter of 1 micron is also universally agreed upon as the size of lowest removal efficiency, with removal increasing as diameter increases or decreases.

## 3.3. Yao's Model

The filtration model derived in Yao et al. (1971) is firstly dependent on the transport model of a suspended particles and the collector (filter media). The three transport mechanisms considered in this model are interception, sedimentation, and diffusion which are represented by A, B, and C respectively in Figure 6 below.

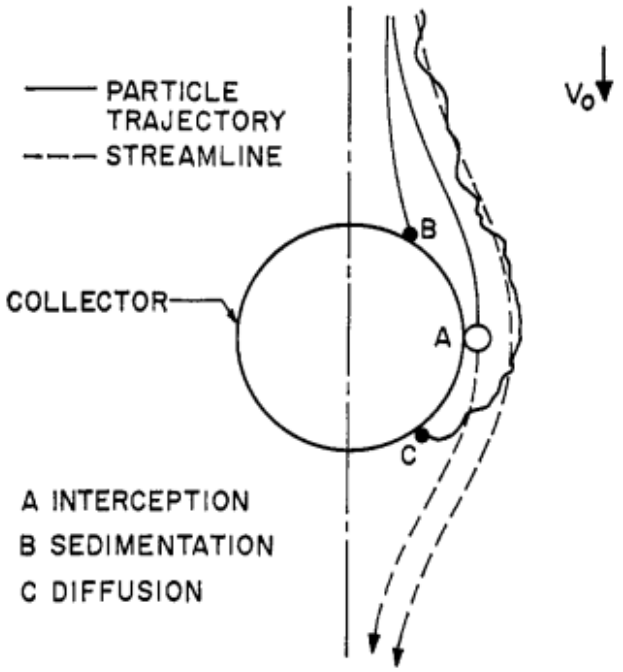


Figure 6. Visual Representation of the 3 Transport Mechanisms (Credit to Yao et al., 1971)

The general equation Yao used to describe the temporal and spatial variation of particle concentration is as follows:

$$\frac{\partial C}{\partial t} + \nu \nabla C = D_{bm} \nabla^2 C + \left(1 - \frac{\rho}{\rho_p}\right) \frac{mg}{3\pi\mu d_p} \frac{\partial C}{\partial z} \quad (1)$$

Where the first term (from left to right) defines the temporal variation of the concentration of particles, second term defines the effects of advection (interception), third term defines the effect of diffusion by Brownian motion (diffusion), and the fourth term defines the effect of gravitational settling (sedimentation).

The form of equation 1 is widely used by engineers for describing the fate of pollutants in any given fluid flow (Yao et al., 1971) and is also applied to filtration processes. Since this equation cannot be solved analytically, the typical approach is to use simplifying

assumptions, one of which being the single-collector efficiency (η). Single-collector efficiency is defined as the ratio of the rate of particles striking the collector over the rate of particles flowing towards the collector, defined as follows:

$$\eta = \frac{rate\ at\ which\ particles\ strike\ collector}{v_o C_o\left(\frac{\pi d^2}{4}\right)} \tag{2}$$

This single collector efficiency was applied to an equation to predict performance of a packed bed. Equation 1 is similar in form to the first order equation used by Iwasaki (1937) and Ives (1960), the integrated form of this equation is as follows:

$$\ln\frac{C}{C_o} = -\frac{3}{2}(1-f)\alpha\eta\left(\frac{L}{d}\right) \tag{3}$$

Further assumptions made in Equation 1 include steady state (dC / dt = 0) and particles are sufficiently small so that Stokes Law applies, which Yao et al. (1971) notes that studies outlined in Spielman and Goren (1970) suggests that assumption is not completely accurate for packed-bed systems. The diffusion coefficient term used was also defined by Einstein's equation:

$$D_{bm} = \frac{kT}{3\pi\mu d_p} \tag{4}$$

Analytically determining the single collector efficiency, efficiency of a single media on removing solids, is the summation of the single-collector efficiencies for all 3 transport

mechanisms. Its important to note that each single-collector efficiency equation derived for each transport mechanism assumes that that transport mechanism is the sole transport mechanism. The individual single-collector efficiencies for each transport mechanisms are as follows:

$$\eta_D = 4.04\, Pe^{-2/3} = 0.9 \left(\frac{kT}{\mu d_p d v_o}\right)^{-2/3} \tag{5}$$

$$\eta_I = \frac{3}{2}\left(\frac{d_p}{d}\right)^2 \tag{6}$$

$$\eta_G = \frac{(\rho_p - \rho) g d_p^2}{18 \mu v_o} \tag{7}$$

The diffusion term was derived in Levich (1962) and the interception and gravitational terms were derived in Yao (1968). The integration of these formulas into a cohesive integrated model is shown in equation 8 where C / Co is the % of particles removed for a given size range.

$$\frac{C}{C_o} = \sum_i^n exp\left(-\frac{3}{2d}(1-f) L\alpha \left(0.9\left(\frac{kT}{\mu d_{p_i} d v_o}\right)^{-\frac{2}{3}} + \frac{3}{2}\left(\frac{d_{p_i}}{d}\right)^2 + \frac{(\rho_p - \rho) g d_{p_i}^2}{18 \mu v_o}\right)\right. \tag{8}$$

## 3.4. Model Implementation

The development of the model begins with inputting Yao's model into a spreadsheet and setting it up in a matrix (by filtration rate and particle size), allowing multiple variables to be changed as needed. Variables required for this model are defined in Table 2.

Table 2. Required Variables for Computing Particle Removal Efficiency

| | | |
|---|---|---|
| Filtration Rate | Input | $m\ h^{-1}$ |
| Media Diameter | Input | m |
| Media Porosity | Input | -- |
| Media Depth | Input | m |
| Particle Density | Input | $kg\ m^{-3}$ |
| Attachment Efficiency | Input | -- |
| Water Density | 998.2 | $kg\ m^{-3}$ |
| Temperature | 293.15 | K |
| Gravitational Const. | 9.81 | $m\ s^{-2}$ |
| Water Viscosity | 0.001 | $kg\ m^{-1}\ s^{-1}$ |
| Boltzmann Constant | 1.381e-23 | $kg\ m^{2}\ s^{-2}\ K^{-1}$ |

The first step in the model is to input the variables for your specific problem you are running. The input table for this model can be seen below in Figure 7.

| Inputtable Constants in Green (do not input in blue cells) | | | |
|---|---|---|---|
| Filtration Rate (m / h) | 10.00 | 10 | up to 100 |
| Media Diameter (mm) | 4 | 4 | Auto Input Values From Table 3 |
| Media Porosity | 0.3 | 0.3 | ☐ |
| Media Bed Depth | 0.621504 | m | no limit |
| Density of Water | 998.2 | kg / m3 | no limit |
| Density of Particle | 1250 | kg / m3 | no limit |
| Attachment Efficiency | 0.5 | -- | 0 - 1 |
| Temperature | 293.15 | K | no limit |

Figure 7. Input Constant Table for Integrated Turbidity Model

In addition to these values, there is also a section where particle size distribution values (by count) is input specific to the problem you are trying to analyze (Figure 8).

| 2 - 5 | 5 -10 | 10 -15 | 15 - 25 | 25 - 50 | 50 - 75 | 75 - 100 | > 100 |
|---|---|---|---|---|---|---|---|
| 2240 | 504 | 361 | 184 | 46 | 12 | 5 | 4 |

Figure 8. Input P-Size Distribution Table for Integrated Turbidity Model

For this table, the values in the upper row of the table are the particle diameter ranges (in micrometers), and the values in the lower row are the number of particles within each size range. The counts shown in this table are the values measured for this example run.

Once these values have all been defined, all you have left to input into the model is the starting turbidity, which is recorded on the output table shown below in Figure 9.

| Turbidity Range | Average expected % removal for various PARTICLE SIZE ranges | | | | | | | | Turbidity of Fluid |
|---|---|---|---|---|---|---|---|---|---|
| 50 - 75 | 2 - 5 | 5 - 10 | 10 - 15 | 15 - 25 | 25 - 50 | 50 - 75 | 75 - 100 | >100 | 55 |
| Estimated Final Turb. | 7.43% | 7.68% | 15.27% | 19.93% | 17.39% | 12.34% | 9.14% | 10.83% | Avg. % contribution |
| 14.194 | 4.087 | 4.222 | 8.399 | 10.960 | 9.564 | 6.788 | 5.024 | 5.956 | Estimated Turbidity |
| CAN NOT | 5.4% | 20.9% | 46.7% | 78.4% | 98.5% | 100.0% | 100.0% | 100.0% | % Removal |
| Achieve <1 NTU | 3.865 | 3.339 | 4.480 | 2.368 | 0.142 | 0.000 | 0.000 | 0.000 | Remaining Turbidity (Rt) |

Figure 9. Output Table for Integrated Turbidity Model

Figure 9 shows the output table where you include the last input (turbidity – in the upper right side) and it predicts the estimated final turbidity value (middle left-hand side).

The calculation step for this final output step first starts of by predicting a particle size ranges % contribution to the turbidity measured (row 3); assuming the total surface area of all the measured particles are linearly related to the measured turbidity value. This assumption was verified in Chapter 2. Therefore, taking the total surface area for all particles in each particle size range as a ratio of the total surface area of all particles can estimate how much of the turbidity is a result of that particular range (row 4).

After relative contribution of each range is established and translated into estimate turbidity values for each size range; the model proposed by Yao can be utilized to estimate the % removal for each size range (by count) and converted over to % removal for each size range (by surface area) (row 5). Taking this removal percentage from each of the size ranges can predict the remaining turbidity from each size range (row 6); taking the summation of all these values leaves you with the final estimated turbidity (middle left-hand side, row 4).

## 3.5. Model Calibration

To calibrate the model, a series of experiments were conducted in the lab to hone in the model's accuracy. Adjustment of the attachment efficiency was done to calibrate the experimental data to the theoretical model prediction.

### 3.5.1. Experimental Setup

The design of the experiment is similar to that used in Altmann et al. (2016), where secondary effluent from a wastewater treatment plant in Germany. The study included a coagulation and flocculation step prior to their granular filtration using GAC and sand media in a 6-inch column. Coagulation / flocculation was not within scope of this experimental evaluation, however the general design of the experiment is very comparable to Altmanns.

For this study, a 264-Liter aquaria tank was used to store the water to be treated; solids were dosed into the tank via Arizona Test Dust. Solids were kept in suspension with a submersible pump (Wayne, GFU110) placed sideways in the tank. Water was pumped out of the tank with a small submersible pump (IMAG-Ph1) placed in a 4-inch column, enclosed in a 100-micron mesh screen. Filtration experiments were run with a 4" column, with the bed depth fixed to 2 feet; testing 3 different media types (Enhanced Nitrification (EN), Standard Media (Std.), and Fine Polyethylene Bead (FPB)) [Appendix E – Media Types]. An overview of this experimental setup can be found in Figure 10.

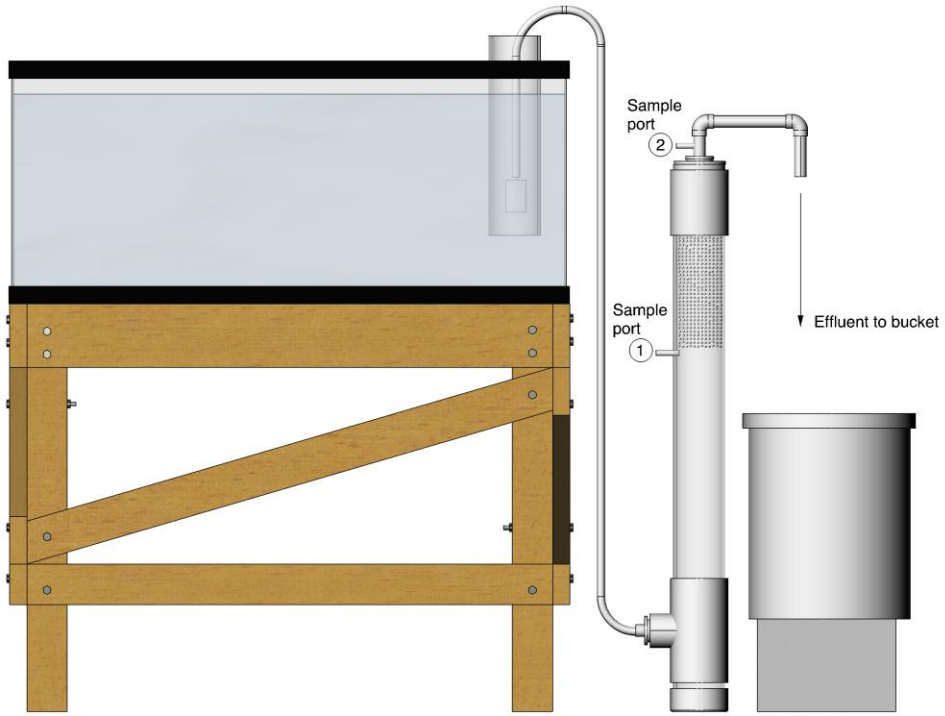


Figure 10. Overview of Experimental Setup to Calibrate Integrated Turbidity Model

### 3.5.2. Experimental Procedure

Experiments were conducted at three different flux rates (1, 2, 3 m $h^{-1}$) for three different media types. Each flux rate was tested three times for each media type with the media being thoroughly cleansed in between each run (n = 27). Flux rates tested were conducted at random to normalize potential continuation errors. Initial particle size and turbidity samples for each measurement were taken right below the media bed. All measurements were taken in triplicate. Sampling procedures were conducted the same as in Chapter 2 – Development of Turbidity Model.

Particle size distribution measurements were conducted with a particle size analyzer (ChemTrac Pc 3400). This flow-through analyzer requires the sample to flow at a rate of 75 ml / min. A peristaltic pump was used to dial in this flow rate and to minimize the effect of particle shearing from pumping. This particle size analyzer does not measure each individual particle size; rather, it measures particles sizes in ranges (ex. 2-5, 5-10, 10-15 microns, etc.). It also measures particles 100 microns and up as ">100", so to minimize reading errors samples were pre-screened with a 100 micron mesh.

Turbidity was measured with a portable turbidimeter (2100Q Portable Turbidimeter). Samples were collected in 15 mL vials. To minimize potential errors from sampling, turbidity samples were taken directly from the outflow of the particle size analyzer to achieve the most accurate correlation between the two measurements. Each vial was thoroughly washed in triplicate between each measurement.

### 3.5.3. Experimental Data

Each experimental run was conducted in triplicate for each media at each flux rate analyzed. Figure 11 below shows an example of before and after particle size counts for 1 run.

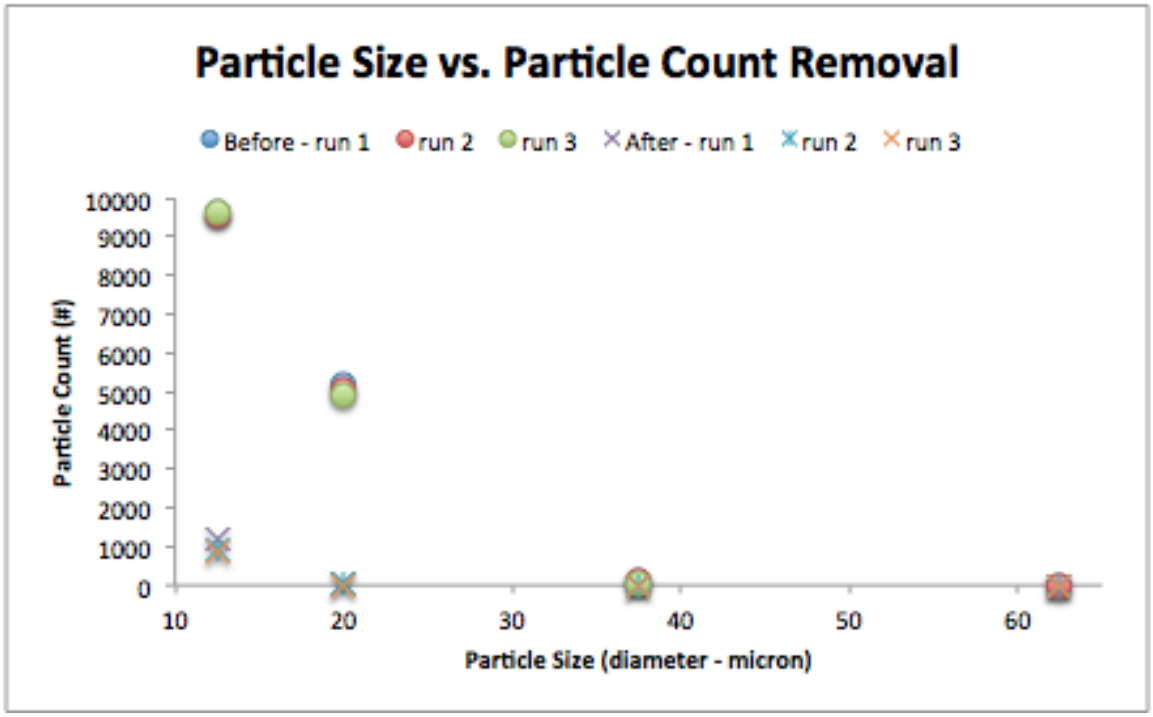

Figure 11. Particle Size vs. Particle Count Removal

Data points below 10-micron diameter particles were removed since they yielded negative removal values, which are possibly a result of an error on the particle size analyzers end as it was a common error seen with all runs. Figure 3 shows the underlying raw data that was averaged to produced all future graphs based on the experimental data, 27 of these figures were created in total for this experiment.

Averaging these points and determining the percentage removal at various media sizes and flux rates can be seen below in Figures 12-14. Data points were also curve fitted.

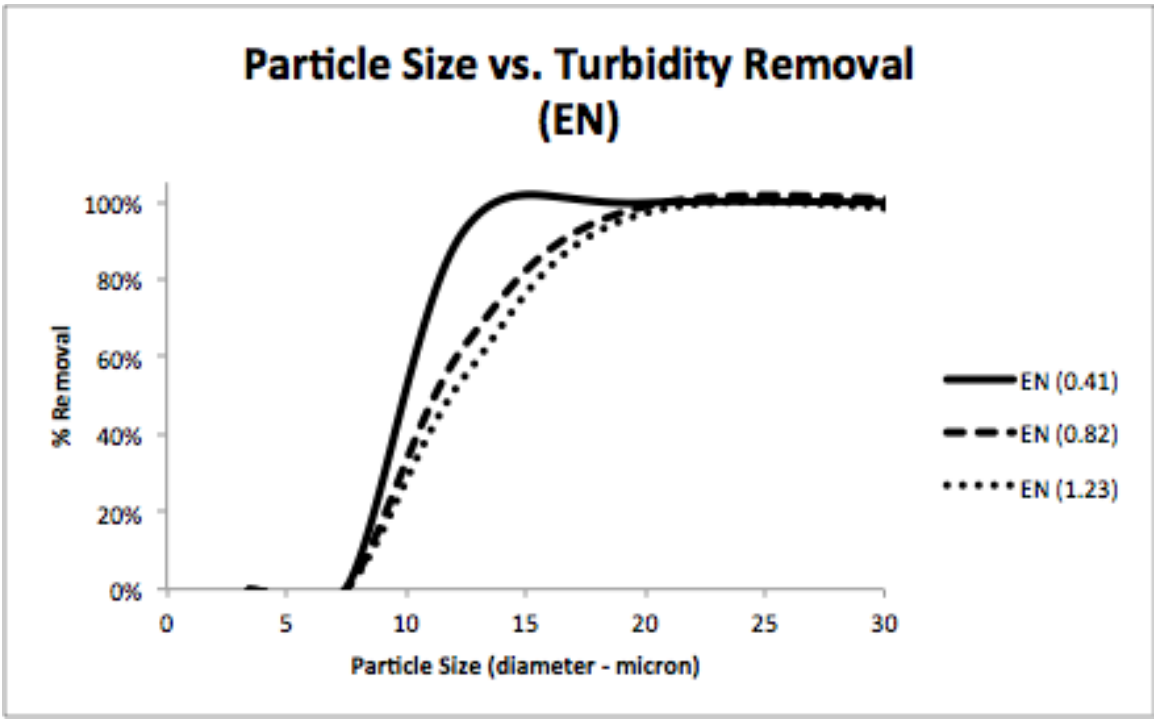


Figure 12. Particle Size vs. Turbidity Removal (EN media). Average % removal in particles as a function of particle size at varying flux rates (1, 2, 3 m $h^{-1}$) for EN media.

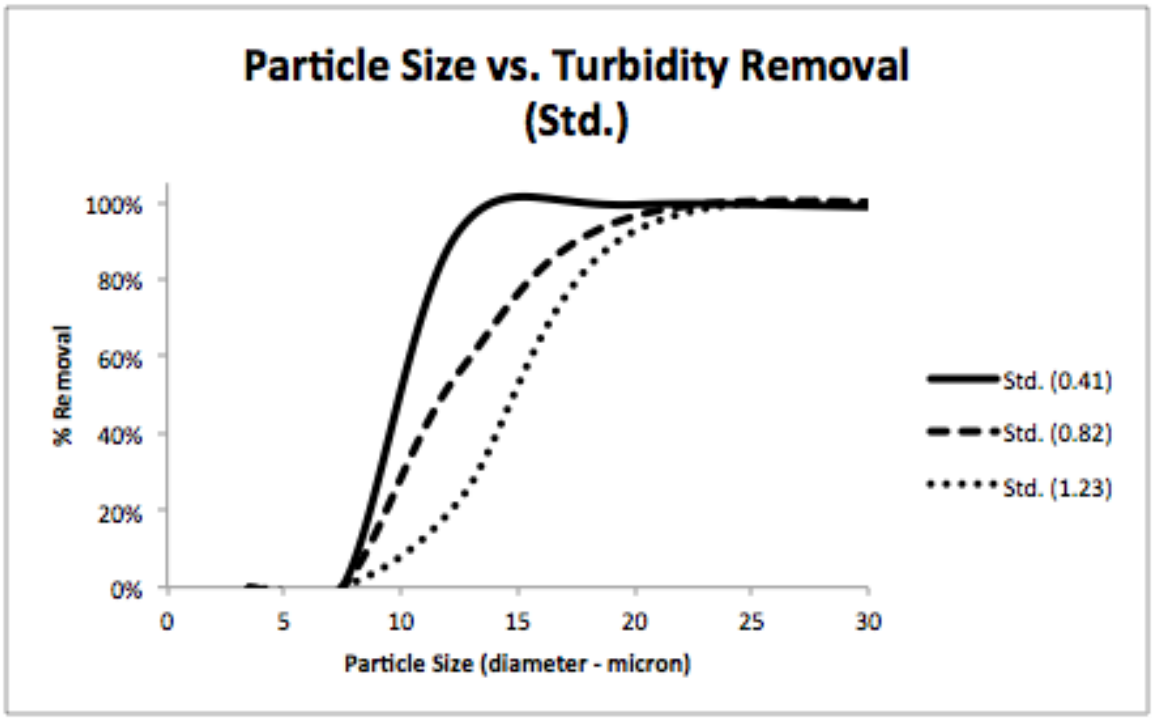


Figure 13. Particle Size vs. Turbidity Removal (Std. media). Average % removal in particles as a function of particle size at varying flux rates (1, 2, 3 m $h^{-1}$) for Std. media.

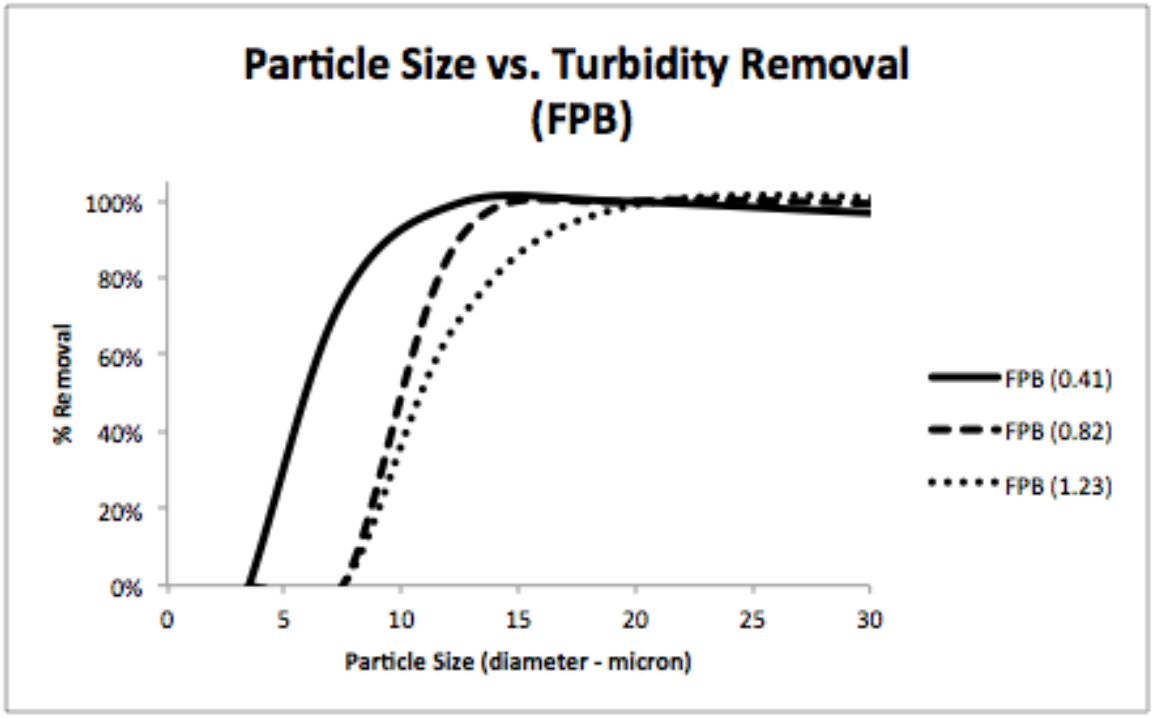


Figure 14. Particle Size vs. Turbidity Removal (FPB media). Average % removal in particles as a function of particle size at varying flux rates (1, 2, 3 m $h^{-1}$) for FPB media.

From Figures (12-14) it can be observed that removal rates are heavily dependent on the flux rate for any given media type. Lowering the flux rate is predicted to allow the granular bed to effectively remove smaller particles. For each media and flux rate tested, particles smaller than five microns were intact. This is likely the result of the limitation on the particle size analyzer used since values below 10 microns consistently returned negative removal rates.

### 3.5.4. Optimal Attachment Efficiency

Yao's Filtration model is derived through a theoretical analysis of solids transport and known science in an ideal world; however, to fit into the real world it included an empirical variable, the attachment efficiency coefficient, which is defined by Yao as the ratio of particle adhesion to the media surface to number of contacts made. To determine

the optimal attachment efficiency, the experimental data was analyzed under varying attachment coefficients (to the nearest $10^{th}$) and evaluated by the mean-squared error from the theoretical prediction and the actual data. The results from this analysis are shown below in Table 3.

Table 3. Mean-Squared Error Between Theoretical Prediction and Actual Data

| Media Type | Attachment Efficiency | | | |
|---|---|---|---|---|
| | 0.4 | 0.5 | 0.6 | 0.7 |
| EN | 215.20 | 126.38 | 96.82 | 106.07 |
| Std. | 112.82 | 42.90 | 66.80 | 120.96 |
| FPB | 45.95 | 23.03 | 60.48 | 128.97 |

From the mean-squared error analysis shown in table 3, it can be seen that an attachment efficiency of 0.6 is best for the EN media while an attachment efficiency of 0.5 is best for both Std. and FPB media (highlighted values). Using these attachment efficiencies to plot the % predicted turbidity removal against varying flux rates can be seen below in Figures 15 – 17. Each figure also includes lines ±10% of the prediction to show how the experimental data points (3 data points for each flux rate) matched up with the theoretical prediction (solid line).

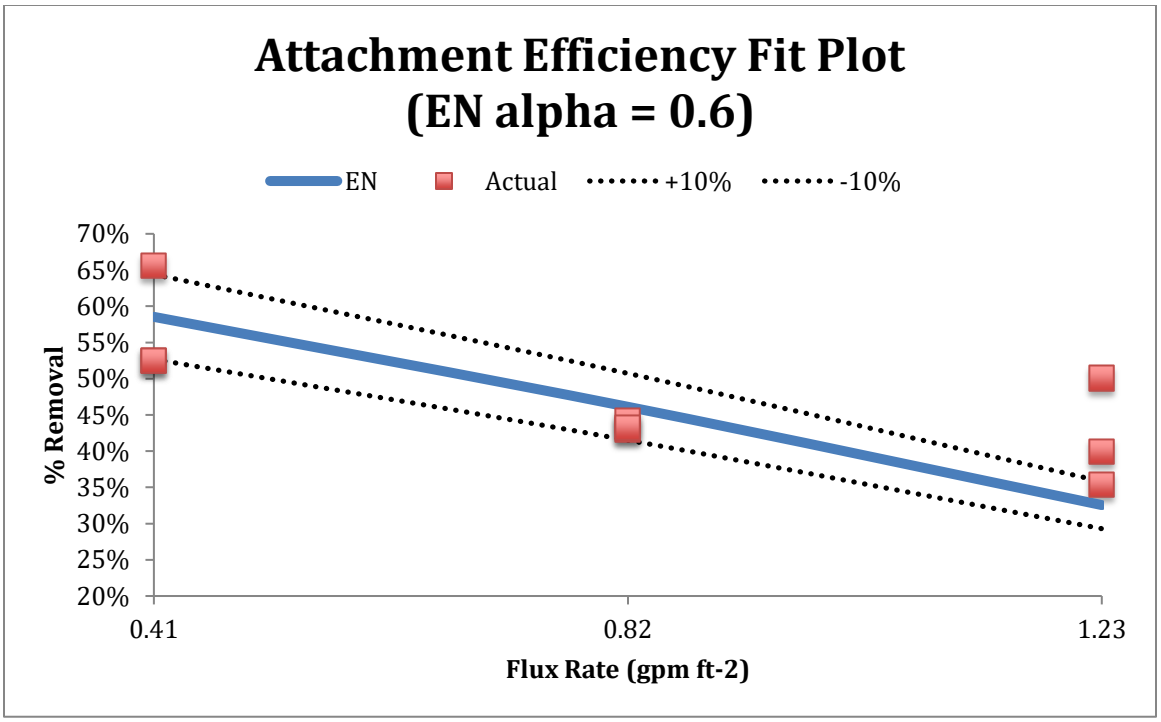


Figure 15. Attachment Efficiency Plot (EN media). Prediction line (±10%) plotted against the experimental data (scattered) for the Enhanced Nitrification Media.

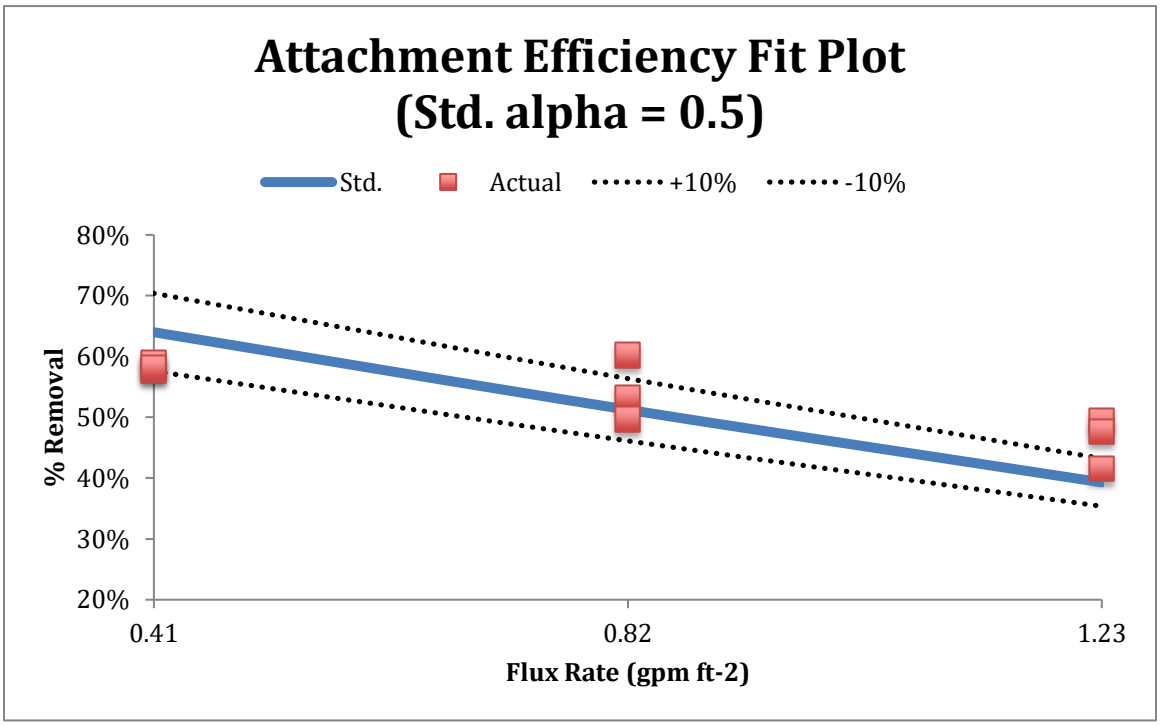


Figure 16. Attachment Efficiency Plot (Std. media). Prediction line (±10%) plotted against the experimental data (scattered) for the Standard Media.

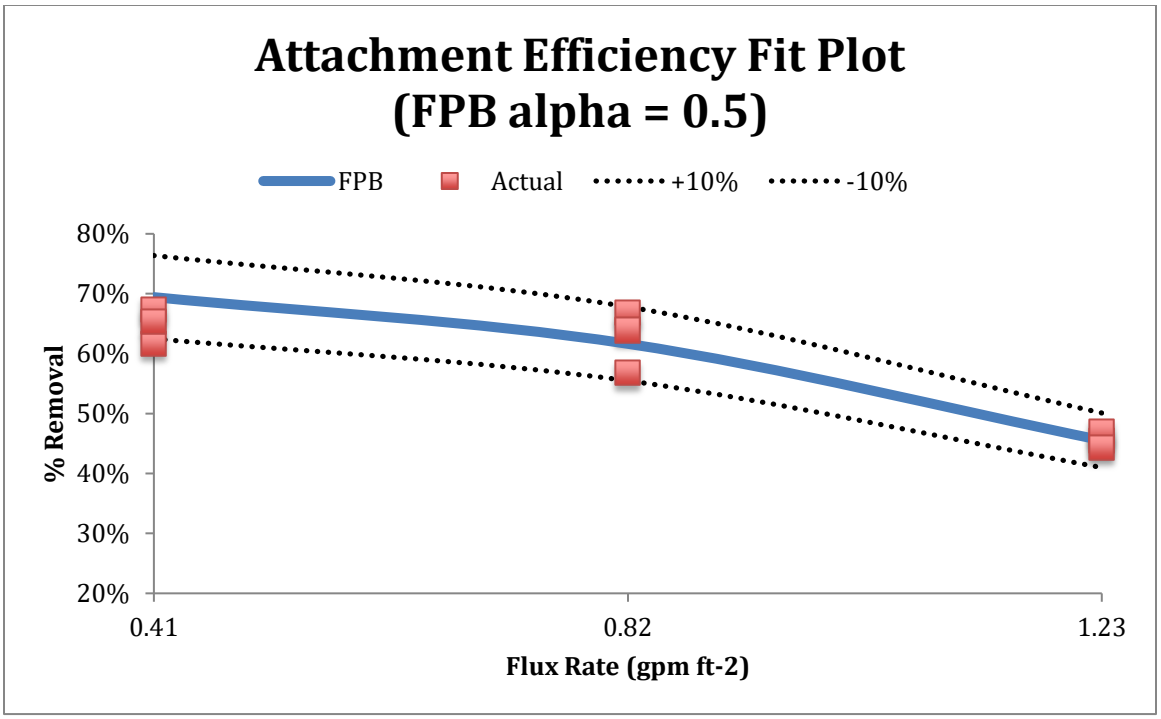


Figure 17. Attachment Efficiency Plot (FPB media). Prediction line (±10%) plotted against the experimental data (scattered) for the Fine Polyethylene Bead.

## 3.6. Sensitivity Analysis

A sensitivity analysis was conducted on the input constants defined on Table 2 to measure the degree to which they affect the final estimated turbidity removal. The default values for the parameters used for the two analyses are shown below in Table 4 and the results from this analysis can be seen below in Figure 18.

Table 4. Default Values for Sensitivity Analysis

| | | |
|---|---|---|
| Filtration Rate | 10 | m h-1 |
| Media Diameter | 4 | m |
| Media Porosity | 0.3 | -- |
| Media Depth | 0.62 | m |
| Particle Density | 1050 | kg m-3 |
| Attachment Efficiency | 0.5 | -- |

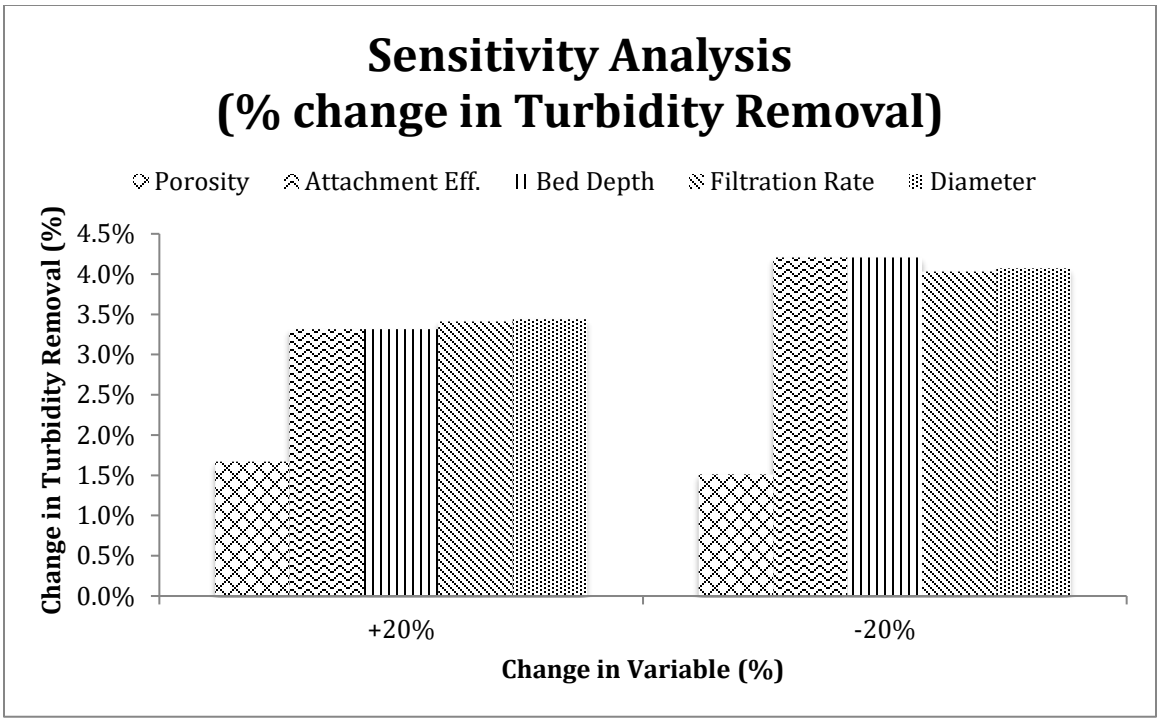


Figure 18. Sensitivity Analysis (% Change in Turbidity Removal). Percentage change in turbidity removal is a function of each individual variable being increased or decreased by 20%.

Figure 18 shows that each input has a relatively equal relationship to the final turbidity removal measurement; however, the model's sensitivity to changes in porosity is half that of the other variables. From this analysis, particle density was removed because of its inconsistent relation between its change and the final turbidity measurement. These large values also skewed the chart and made it difficult to actually see any relations. An individual sensitivity analysis was conducted for just the particle density, which can be seen below in Figure 19.

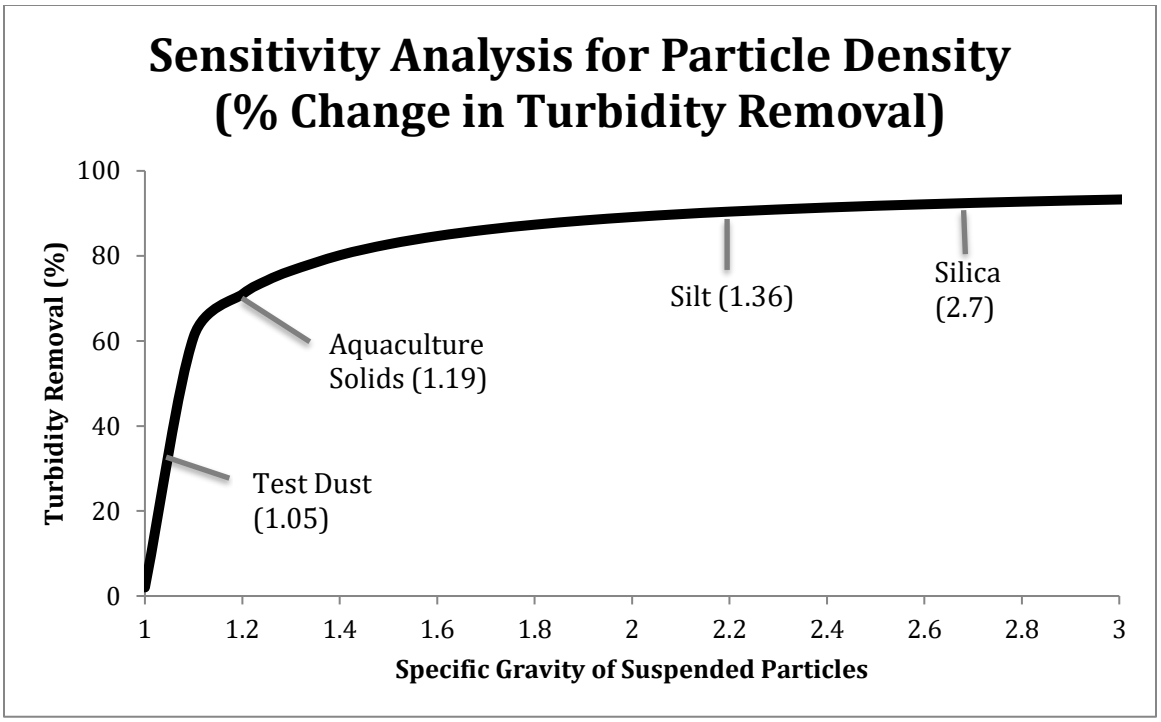


Figure 19. Sensitivity Analysis for Particle Density (% Change in Turbidity Removal). Aquaculture Solids specific gravity (SG) from Chen et al. 1993

Figure 19 plots expected turbidity removal against the specific gravity of the particle. The test dust point shows the default point of analysis conducted for the first sensitivity analyses (shown in Table 4). From this point, raising and lowering the density by 20%, as conducted in the first analysis, produces two widely different answers. Due to the nature of the equations used for this model, particle densities lower than the water density produced negative results and the model results become extremely sensitive to very small changes in particle density as the two densities approach one another.

Removal efficiency is also very dependent on the size of the particle, which is then heavily influenced by the filtration rate. Removal rates of around 100% can be achieved for particles >10 microns in diameter simply by lowering the filtration rate to 1 m/h. However, small particle sizes (< 5 microns) prove very difficult to remove, even at low

filtration rates. Figure 20 shows the sensitivity of particle removal by varying filtration rates.

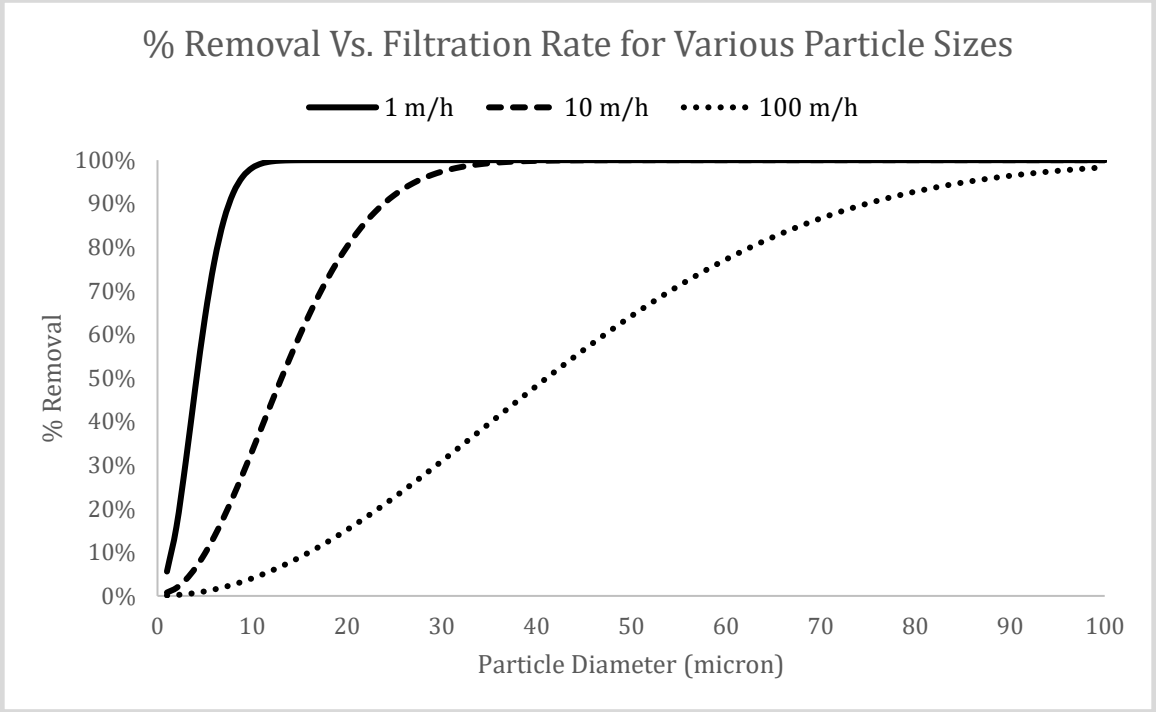


Figure 20. % Removal vs. Filtration Rate for Various Particle Sizes. Effectiveness of the granular bed on various particle sizes at 3 different filtration rates. (media diameter = 4mm, bed porosity = 30%, bed depth = 0.62m, attachment efficiency = 0.5, Temperature = 293 K, particle density = 1250 kg $m^{-3}$, water density = 998.2 kg $m^{-3}$)

## 3.7. Discussion

Combining the Turbidity Model with Yao's Filtration Model yielded an integrated model capable of predicting the effectiveness of turbidity removal from a granular bed relatively accurately once adjusted to the optimal attachment efficiency. Standard and the FPB media showed fairly expected results, with % removal declining fairly linearly with increasing flux. EN media however showed a variation from those media types with a somewhat upward curve towards the end of the flux range measured (figure 15). This is most likely due to the shape of the media, since the Std. and FPB medias are both fairly

spherical while the EN media is crimped [Appendix B – Experimental Setup for Calibration]. This crimping essentially provides a zone for solids to reside in without being subjected to the full strength of the streamline flow, which could result in higher removal efficiencies over the un-crimped media.

For overall turbidity removal, the effectiveness of each media type (from best to worst) would be FPB, Std., and then EN. This is expected since the smaller media would allow for higher removal rates for interception. So when designing a granular bed to remove turbidity you would want the granular media to be a small as practically possible. Limitations on minimizing the size of the media would primarily be due to biofouling or excess energy demands for flow through the bed.

After analyzing the attachment efficiency for each media, it seems the best attachment efficiency for the clean media types tested lies somewhere between 0.5 and 0.6. This difference is likely due to the difference in shape as the fairly spherical media types were around 0.5 and the crimped EN media was 0.6. However, EN media also has a higher porosity when compared to both the standard and FPB, so it is not clear that just the shape was the cause of better removal; the effect of porosity can be seen in equation 3. These attachment efficiencies are likely to be conservative estimates from what one would expect in the field since a biofilm is likely to grow on the media. A biofilm would be expected to make the surface of the media sort of sticky, which would increase the attachment efficiency. In addition, biofilm growth would also lower the porosity of the bed increasing the overall effectiveness even further.

After conducting the sensitivity analysis on the model it was shown that flux rate and particle density have the largest impact on expected turbidity removal from a granular bed. Lower flux rates and denser particles yielded better results. Out of the two however, particle density seems to be the most influential. It is also important to note that removal rates conducted in this study are highly conservative since the particle density analyzed during the laboratory experiments were extremely low compared to particle densities seen in practice. For the study, Arizona Test Dust was used, which has a particle density of 1.05 kg / L where the lowest particle densities seen in practice (from aquaculture solids) are around 1.19 kg / L (Figure 19).

## 3.8. Conclusion

After developing the Integrated Turbidity Removal Model and calibrating it with experimental data, it seems to be a fairly accurate indicator on what you can expect your designed granular bed to remove, in terms of turbidity for dilute solids loads (representative of surface waters). Using this model also shows promise in highlighting the key parameters to focus on when designing a filtration system, most notably including: Particle density, filtration rate (flux rate), and media size. Most effective media for removing turbidity during this study were FPB, Std., and then EN. Expected attachment efficiencies for the clean medias tested are around 0.5 to 0.6.

# Chapter 4. Conclusion

## 4.1. Conclusions

The assumption that turbidity is linearly dependent on the available surface area of suspended particles is valid, at least within a turbidity range of 0 – 100 NTU. Taking this relation and applying it to Yao's Filtration Model yields a model that is reasonably accurate at determining the effectiveness of a granular bed on removing turbidity from a given water source. Moving forward, this model can be useful to design engineers to aid in the design of filtration systems to achieve desired turbidity goals.

## 4.2. Recommendations

My recommendations for future students pursing this topic in their field of study would be as followed:

1. A more rigorous mathematical derivation for the Integrated Turbidity Removal Model.
2. How does flux rate, particle size, or media size/shape effect attachment efficiency?
3. What is the best way to determine attachment efficiency and how can a media be engineered to achieve the maximum efficiency?
4. How, or to what degree, does biofilm development on a media's surface effect its attachment efficiency
5. An evaluation of different water sources, such as municipal / residential wastes

Along with these recommendations, future studies conducted to verify or improve upon the model in its current standing would also be a useful endeavor to pursue.

# References


Altmann, J., Rehfeld, D., Träder, K., Sperlich, A., and Jekel, M. 2016. Combination of granular activated carbon adsorption and deep-bed filtration as a single advanced wastewater treatment step for organic micropollutant and phosphorus removal, Water Research, Volume 92, Pages 131-139, ISSN 0043-1354

Baker, M. N. 1949. The quest for pure water: the history of water purification from the earliest records to the twentieth century. New York: American Water Works Association.

Bergheim, A., Kristiansen, R., and Kelly, L.A. 1993a. Treatment and utilization of sludge from landbased farms for salmon. In: Wang, J.-W. (Ed.), Techniques for Modern Aquaculture. Proceedings of an Aquaculture Engineering Conference, 21–23 June 1993, Spokane, WA. American Society of Agriculture Engineers, St. Joseph, MI, pp. 486–495.

Chen, S., Timmons, M. B., Aneshansley, D. J., and Bisogni. J. J. 1993. Suspended solids characteristics from recirculating aquacultural systems and design implications, Aquaculture, Volume 112, Issues 2–3, Pages 143-155, ISSN 0044-8486.

Chesness, J. L., Poole, W. H., and Hill, T. K. 1975. Settling basin design for raceway fish production systems. Trans. ASAE 18, 159–162.

Chiang, H. C., and Lee, J. C. 1986. Study of treatment and reuse of aquacultural wastewater. Aquacultural Engineering 5, 301 – 312.

Cookson, K. T., Jr. 1970. Removal of submicron particles in packed beds. Environmental Science Technology 4, 128 – 134.

Cripps, S. J. 1993. The application of suspended particle characterization techniques to aquaculture systems. In: Wang, J. (Ed.), Techniques for modern aquaculture. Proceedings of an Aquacultural Engineering Conference, 21 – 23 June 1993, Spokane, WA. American Society of Agricultural Engineers, St. Joseph, MI 26 - 34.

Cripps, S. J., and Bergheim, A. 2000. Solids management and removal for intensive land-based aquaculture production systems. Aquaculture Engineering 22, 33 – 56.

Cripps, S. J., and Kelly, L. A. 1996. Reductions in wastes from aquaculture, Aquaculture and Resource Management 16 – 201

Environmental Protection Agency (EPA). 2018. “National Primary Drinking Water Regulations.” www.epa.gov/ground-water-and-drinking-water/national-primary-drinking-water-regulations.

Friedlander, S. K. 1958. Ind. Engineering Chemical 50, 1161 – 1164.

Hach. 2018. "Turbidity." *Hach.com*, https://www.hach.com/asset-get.download-en.jsa?id=7639984265.

Healy, M. G., and Rodgers, M. 2007. Treatment of dairy wastewater using constructed wetlands and intermittent sand filters. Bioresource Technology 98, 2268 – 2281.

Huguenin, J. E., and Colt, J. 1989. Design and Operating Guide for Aquaculture Seawater Systems, Elsevier, Amsterdam, p. 264

Ives, K. J. 1960. Rational design of filters. Proc. Institute of Civil Engineering. 16, 189 – 193.

Iwasaki, T. J. 1937. Some notes on sand filtration. American Water Works Association 29, 1591 – 1597.

Lawson, T. B. 1994. Fundamentals of aquaculture engineering. Chapman and Hall, New York. 355.

Levich, V. G. 1962. Physiochemical hydrodynamics, Prentice Hall, Englewood Cliffs, N. J., 80 – 85.

Louden, T. L., Thompson, D. B., Fay, L., and Reese, L. E. 1985. Cold-Climate Performance of Recirculating Sand Filters. In Proceedings of the Fourth On-site Wastewater Treatment Symposium. American Society of Agricultural Engineers, St. Joseph, MI.

Mäkinen, T., Lindgren, S., and Eskelinen. P. 1988. Sieving as an effluent treatment method for aquaculture. Aquacult. Eng., 7, 367-377

Malone, R. F., and Beecher, L. E. 2000. Use of floating bead filters to recondition recirculating waters in warm water aquaculture production systems. Aquaculture Eng. 22: 57 – 73.

Malone, R. F., and Gudipati, S. 2007. Airlift-PolyGeyser combination facilitates decentralized water treatment in recirculating marine hatchery systems. Proceedings of the 34th US Japan natural resources panel Aquaculture Symposium, San Diego, California. NOAA technical memorandum NMFS-F/SPO-85.

Owen, J. E., and Bobb, K. L. 1994. Winter Operation and Performance of a Recirculating Sand Filter. In Proceedings of the WEFTEC 67th Annual Conference. Water Environment Federation, Alexandria, VA.

Piluk, R. J., and Peters, E. C. 1994. Small Recirculating Sand Filters for Individuals Homes. In Proceedings of the Seventh On-site Wastewater Treatment Symposium. American Society of Agricultural Engineers, Joseph, MI.

Roy, C., and Dube, J. P. 1994. A Recirculating Gravel Filter for Cold Climates. In Proceedings of the Seventh On-site Wastewater Systems Symposium. American Society of Agricultural Engineers, St. Joseph, MI.

Smoluchowski, V. M. 1917. Versucheiner mathematischen theorie der koagulation kinetic kolloide lousungen Z. The Journal of Physical Chemistry 92, 129 – 168.

Spielman, L. A., and Goren, S. L. 1970. Capture of small particles by London forces from low speed liquid flows. Environmental Sciences Technology 4, 135 – 140.

Tchobanoglous, G., and Burton, F. L. 1991. Wastewater Engineering: Treatment, Disposal and Reuse (3rd edn), McGraw-Hill, New York, p. 1334

Twarowska, J. G., Westerman, P. W., and Losordo, T. M. 1997. Water Treatment and Waste Characterization Evaluation of an Intensive Recirculating Fish Production System. Aquaculture Engineering, 16, pp. 133-147

Visvanathan, C., Werellagama, D. R. I. B., and Ben Aim, R. 1996. Surface water pretreatment using floating media filter. Environmental Engineering Journal, 25 – 33.

Weaver, L., Pfieffer, T., and Malone, R. 2018. USDA SBIR Biofloc Phase 1 Report.

Weber, W. J. 1972. Physiochemical processes for water quality control, Wiley-Interscience, New York. 111 – 138.

Wheaton, F. W. 1977. Aquacultural Engineering, Wiley, Chichester, UK

World Health Organization (WHO). 2018. “Guidelines for Drinking Water Quality.” WHO.int, www.who.int/water_sanitation_health/dwq/gdwqvol32ed.pdf.

Yao, K. M. 1968. “Influence of suspended particle size on the transport aspect of water filtration,” unpublished Ph.D. dissertation, University of North Carolina, Chapel Hill, N.C.

Yao, K. M., Habibian, M. T., and O'Melia, C. R. 1971. Water and waste water filtration. Concepts and applications Environmental Science and Technology 5 (11), 1105-1112 DOI: 10.1021/es60058a005

# Appendix A. Table of Variables

| Variable | Name | Units |
|---|---|---|
| $\alpha$ | Attachment Efficiency | -- |
| L | Bed Depth | m |
| k | Boltzmann's Constant | kg $m^2$ $s^{-2}$ $K^{-1}$ |
| $D_{bm}$ | Brownian Motion Diff. | -- |
| C | Concentration | mg $L^{-1}$ |
| $C_o$ | Concentration Initial | mg $L^{-1}$ |
| $\rho_p$ | Density Particle | kg $m^{-3}$ |
| $\rho$ | Density Water | kg $m^{-3}$ |
| d | Diameter Media | m |
| $d_p$ | Diameter Particle | m |
| $\eta$ (I, S, D) | Single Collector Eff. | -- |
| g | Gravity | m $s^{-2}$ |
| $\mu$ | Kinematic Viscosity | kg $m^{-1}$ $s^{-1}$ |
| m | Mass of Particle | kg |
| Pe | Peclet Number | -- |
| *f* | Porosity of Media Bed | -- |
| T | Temperature | K |
| t | Time | s |
| $\nu$ | Velocity | m $s^{-1}$ |
| z | Vertical Height | m |

# Appendix B. Experimental Setup


Figure B.1. Shows the peristaltic pump (on the right) connected to the particle size analyzer (ChemTrac PC 3400 – on left) used for this study. Peristaltic pump was used to gently flow samples to be measured through the particle size analyzer. The particle size analyzer was used to measure the particle size distribution of the samples.


Figure B.2. Shows the Turbidimeter (HACH 2100Q) as well as the 15 mL sample vials used for this study. Turbidimeter was used to collect turbidity measurements of samples taken.

# Appendix C. Raw Data

| University Lake | Raw | | | Alum added (fast mix) | | | Alum added (slow mix) | | | Settled | | |
|---|---|---|---|---|---|---|---|---|---|---|---|---|
| 2 - 5 µm | 1126 | 1210 | 1242 | 942 | 884 | 870 | 910 | 935 | 956 | 3634 | 3609 | 3645 |
| 5 -10 µm | 4398 | 4569 | 4692 | 3115 | 2959 | 2944 | 3127 | 3134 | 3171 | 10644 | 10676 | 10640 |
| 10 -15 µm | 7215 | 7537 | 7596 | 4773 | 4751 | 4836 | 4977 | 4960 | 4958 | 9669 | 9641 | 9566 |
| 15 - 25 µm | 8934 | 9002 | 8900 | 8059 | 8469 | 8678 | 8573 | 8538 | 8478 | 2160 | 2098 | 2069 |
| 25 - 50 µm | 3116 | 2809 | 2561 | 5414 | 5554 | 5638 | 5312 | 5288 | 5216 | 112 | 89 | 102 |
| 50 - 75 µm | 548 | 374 | 319 | 807 | 784 | 738 | 700 | 703 | 702 | 18 | 12 | 20 |
| 75 - 100 µm | 162 | 80 | 82 | 188 | 178 | 165 | 143 | 147 | 148 | 1 | 0 | 1 |
| > 100 µm | 89 | 21 | 47 | 82 | 81 | 69 | 56 | 52 | 53 | 1 | 0 | 1 |
| Turbidity (NTU) | 65.9 | 70.5 | 70 | 232 | 179 | 163 | 74.3 | 74.8 | 78.1 | 18.8 | 19.6 | 18.9 |

| (North) Capitol Lake | Raw | | | Alum added (fast mix) | | | Alum added (slow mix) | | | Settled | | |
|---|---|---|---|---|---|---|---|---|---|---|---|---|
| 2 - 5 µm | 2926 | 3021 | 3039 | 2662 | 2469 | 2319 | 2364 | 2437 | 2448 | 7837 | 7489 | 7370 |
| 5 -10 µm | 8924 | 9036 | 9040 | 4434 | 4504 | 4519 | 4546 | 4577 | 4574 | 3451 | 3259 | 3264 |
| 10 -15 µm | 9465 | 9476 | 9374 | 4765 | 5011 | 5233 | 5251 | 5270 | 5247 | 711 | 690 | 767 |
| 15 - 25 µm | 4436 | 4339 | 4199 | 5825 | 6089 | 6382 | 6437 | 6343 | 6257 | 256 | 259 | 333 |
| 25 - 50 µm | 630 | 542 | 522 | 2239 | 2220 | 2216 | 2287 | 2209 | 2204 | 33 | 32 | 83 |
| 50 - 75 µm | 124 | 98 | 97 | 224 | 218 | 215 | 213 | 204 | 198 | 2 | 4 | 19 |
| 75 - 100 µm | 43 | 27 | 34 | 51 | 43 | 43 | 42 | 41 | 36 | 0 | 1 | 8 |
| > 100 µm | 26 | 12 | 15 | 23 | 14 | 20 | 14 | 11 | 11 | 1 | 2 | 8 |
| Turbidity (NTU) | 17.5 | 16.4 | 17.9 | 20.5 | 21.5 | 20.5 | 19.7 | 18.4 | 18.2 | 2.78 | 3.15 | 2.74 |

| Mississippi River | Raw | | | Alum added (fast mix) | | | Alum added (slow mix) | | | Settled | | |
|---|---|---|---|---|---|---|---|---|---|---|---|---|
| 2 - 5 µm | 389 | 530 | 494 | 261 | 233 | 208 | 343 | 407 | 377 | 7198 | 6878 | 6794 |
| 5 -10 µm | 1692 | 2189 | 1673 | 1193 | 964 | 991 | 1555 | 2184 | 2051 | 4500 | 3506 | 3535 |
| 10 -15 µm | 3473 | 4442 | 3282 | 2639 | 2071 | 2248 | 3295 | 4757 | 4439 | 2468 | 1654 | 1637 |
| 15 - 25 µm | 9149 | 10731 | 7323 | 7378 | 6181 | 6846 | 8722 | 11113 | 10350 | 2164 | 1500 | 1490 |
| 25 - 50 µm | 10000 | 7921 | 6993 | 10263 | 10771 | 11246 | 10019 | 7998 | 7568 | 589 | 405 | 413 |
| 50 - 75 µm | 1258 | 371 | 1702 | 2548 | 3436 | 2986 | 1755 | 740 | 735 | 24 | 25 | 37 |
| 75 - 100 µm | 135 | 13 | 503 | 685 | 840 | 664 | 319 | 131 | 144 | 5 | 7 | 12 |
| > 100 µm | 22 | 2 | 246 | 260 | 276 | 237 | 99 | 59 | 89 | 4 | 4 | 10 |
| Turbidity (NTU) | 92.7 | 98.6 | 96.1 | 189 | 172 | 169 | 62.3 | 62.8 | 56.6 | 12.7 | 8.88 | 12.2 |

| City Park Lake | Raw | | | Alum added (fast mix) | | | Alum added (slow mix) | | | Settled | | |
|---|---|---|---|---|---|---|---|---|---|---|---|---|
| 2 - 5 µm | 1257 | 1131 | 1299 | 1214 | 1083 | 971 | 1018 | 1028 | 1051 | 8775 | 8693 | 8929 |
| 5 -10 µm | 4772 | 4255 | 4937 | 3083 | 2858 | 2680 | 2742 | 2742 | 2783 | 12522 | 12301 | 12447 |
| 10 -15 µm | 7606 | 6839 | 7761 | 3633 | 3651 | 3643 | 3781 | 3785 | 3769 | 2787 | 2828 | 2701 |
| 15 - 25 µm | 8861 | 8691 | 8854 | 6203 | 6598 | 6884 | 6982 | 6987 | 6940 | 976 | 1059 | 886 |
| 25 - 50 µm | 2890 | 3469 | 2639 | 5803 | 6204 | 6409 | 6262 | 6214 | 6110 | 226 | 265 | 166 |
| 50 - 75 µm | 470 | 687 | 388 | 1119 | 1099 | 1065 | 966 | 945 | 945 | 48 | 66 | 32 |
| 75 - 100 µm | 125 | 222 | 96 | 223 | 194 | 190 | 175 | 156 | 164 | 20 | 28 | 15 |
| > 100 µm | 50 | 128 | 38 | 67 | 62 | 52 | 48 | 43 | 50 | 21 | 20 | 16 |
| Turbidity (NTU) | 52.4 | 50.9 | 51 | 60 | 62.6 | 59.9 | 65.7 | 73.8 | 69.6 | 3.51 | 3.36 | 3.36 |

| (South) Capitol Lake | Raw | | | Alum added (fast mix) | | | Alum added (slow mix) | | | Settled | | |
|---|---|---|---|---|---|---|---|---|---|---|---|---|
| 2 - 5 µm | 2324 | 2433 | 2560 | 1407 | 1368 | 1308 | 552 | 1433 | 1454 | 5552 | 4943 | 3406 |
| 5 -10 µm | 7443 | 7658 | 8037 | 3607 | 3642 | 3610 | 1430 | 3725 | 3741 | 3002 | 2645 | 3282 |
| 10 -15 µm | 9148 | 9293 | 9454 | 5066 | 5179 | 5234 | 2073 | 5220 | 5145 | 1206 | 1143 | 2662 |
| 15 - 25 µm | 5676 | 5616 | 5371 | 7359 | 7661 | 7888 | 3454 | 7643 | 7614 | 664 | 874 | 2581 |
| 25 - 50 µm | 1341 | 1156 | 959 | 4232 | 4287 | 4296 | 2630 | 4102 | 4011 | 270 | 461 | 1063 |
| 50 - 75 µm | 315 | 216 | 150 | 396 | 374 | 362 | 505 | 339 | 313 | 58 | 78 | 104 |
| 75 - 100 µm | 94 | 67 | 35 | 47 | 41 | 40 | 170 | 34 | 35 | 25 | 28 | 22 |
| > 100 µm | 47 | 47 | 20 | 9 | 9 | 8 | 148 | 8 | 6 | 28 | 25 | 14 |
| Turbidity (NTU) | 18.1 | 17.5 | 17.7 | 30.4 | 29.6 | 28.2 | 25.5 | 28.1 | 29.7 | 6.28 | 4.98 | 5.95 |

| | Bayou Duplanier | | | Bayou Plaqumine | | | Other side of Mississippi | | |
|---|---|---|---|---|---|---|---|---|---|
| 2 - 5 µm | 2747 | 2752 | 2765 | 2191 | 2230 | 2232 | 584 | 510 | 525 |
| 5 -10 µm | 8796 | 8691 | 8765 | 7031 | 7111 | 7221 | 2480 | 2236 | 2274 |
| 10 -15 µm | 8967 | 9000 | 8968 | 8455 | 8498 | 8472 | 5281 | 4774 | 4878 |
| 15 - 25 µm | 3531 | 3659 | 3569 | 5704 | 5665 | 5499 | 11100 | 10717 | 10898 |
| 25 - 50 µm | 179 | 205 | 186 | 855 | 800 | 743 | 4628 | 5725 | 5387 |
| 50 - 75 µm | 3 | 4 | 3 | 34 | 30 | 28 | 75 | 177 | 157 |
| 75 - 100 µm | 0 | 1 | 0 | 6 | 3 | 3 | 2 | 11 | 8 |
| > 100 µm | 0 | 0 | 0 | 0 | 0 | 0 | 0 | 1 | 1 |
| Turbidity (NTU) | 15.8 | 15.5 | 15.3 | 17.5 | 16.8 | 16.7 | 87.7 | 90.6 | 86.5 |

| Monte | | | Comitte | | |
|---|---|---|---|---|---|
| 8931 | 8848 | 8895 | 5640 | 5405 | 5526 |
| 2501 | 2445 | 2422 | 10203 | 9829 | 10028 |
| 530 | 520 | 496 | 4998 | 5161 | 5057 |
| 228 | 207 | 189 | 2199 | 2496 | 2341 |
| 52 | 44 | 38 | 413 | 580 | 493 |
| 4 | 3 | 2 | 27 | 50 | 37 |
| 1 | 0 | 0 | 2 | 8 | 5 |
| 0 | 0 | 0 | 0 | 1 | 1 |
| 7.54 | 6.01 | 6.58 | 24.9 | 25 | 23.1 |

## Appendix D. Graphical Illustrations of Statistical Regression Analysis

The SAS System

The REG Procedure
Model: MODEL2
Dependent Variable: NTU

Number of Observations Read 10

Number of Observations Used 10

Analysis of Variance

| Source | DF | Sum of Squares | Mean Square | F Value | Pr > F |
|---|---|---|---|---|---|
| Model | 1 | 996.81990 | 996.81990 | 0.90 | 0.3715 |
| Error | 8 | 8898.43079 | 1112.30385 | | |
| Corrected Total | 9 | 9895.25069 | | | |

| | | | |
|---|---|---|---|
| Root MSE | 33.35122 | R-Square | 0.1007 |
| Dependent Mean | 40.29100 | Adj R-Sq | -0.0117 |
| Coeff Var | 82.77585 | | |

Parameter Estimates

| Variable | DF | Parameter Estimate | Standard Error | t Value | Pr > \|t\| |
|---|---|---|---|---|---|
| Intercept | 1 | -19.04025 | 63.55510 | -0.30 | 0.7721 |
| Count | 1 | 0.00250 | 0.00264 | 0.95 | 0.3715 |

Figure D.1. shows the SAS regression model output for count of particles versus turbidity.

The SAS System

The REG Procedure
Model: MODEL3
Dependent Variable: NTU

Number of Observations Read 10

Number of Observations Used 10

Analysis of Variance

| Source | DF | Sum of Squares | Mean Square | F Value | Pr > F |
|---|---|---|---|---|---|
| Model | 1 | 8293.66739 | 8293.66739 | 41.43 | 0.0002 |
| Error | 8 | 1601.58330 | 200.19791 | | |
| Corrected Total | 9 | 9895.25069 | | | |

| | | | |
|---|---|---|---|
| Root MSE | 14.14913 | R-Square | 0.8381 |
| Dependent Mean | 40.29100 | Adj R-Sq | 0.8179 |
| Coeff Var | 35.11735 | | |

Parameter Estimates

| Variable | DF | Parameter Estimate | Standard Error | t Value | Pr > \|t\| |
|---|---|---|---|---|---|
| Intercept | 1 | 0.71974 | 7.60382 | 0.09 | 0.9269 |
| SA | 1 | 1.45253 | 0.22567 | 6.44 | 0.0002 |

Figure D.2. shows the SAS regression model output for surface area of particles versus turbidity.

The SAS System

The REG Procedure
Model: MODEL4
Dependent Variable: NTU

Number of Observations Read 10

Number of Observations Used 10

**Analysis of Variance**

| Source | DF | Sum of Squares | Mean Square | F Value | Pr > F |
|---|---|---|---|---|---|
| Model | 1 | 7487.60299 | 7487.60299 | 24.88 | 0.0011 |
| Error | 8 | 2407.64770 | 300.95596 | | |
| Corrected Total | 9 | 9895.25069 | | | |

| | | | |
|---|---|---|---|
| Root MSE | 17.34808 | R-Square | 0.7567 |
| Dependent Mean | 40.29100 | Adj R-Sq | 0.7263 |
| Coeff Var | 43.05697 | | |

**Parameter Estimates**

| Variable | DF | Parameter Estimate | Standard Error | t Value | Pr > \|t\| |
|---|---|---|---|---|---|
| Intercept | 1 | 11.40625 | 7.97687 | 1.43 | 0.1906 |
| Volume | 1 | 0.17690 | 0.03547 | 4.99 | 0.0011 |

Figure D.3. shows the SAS regression model output for volume of particles versus turbidity.

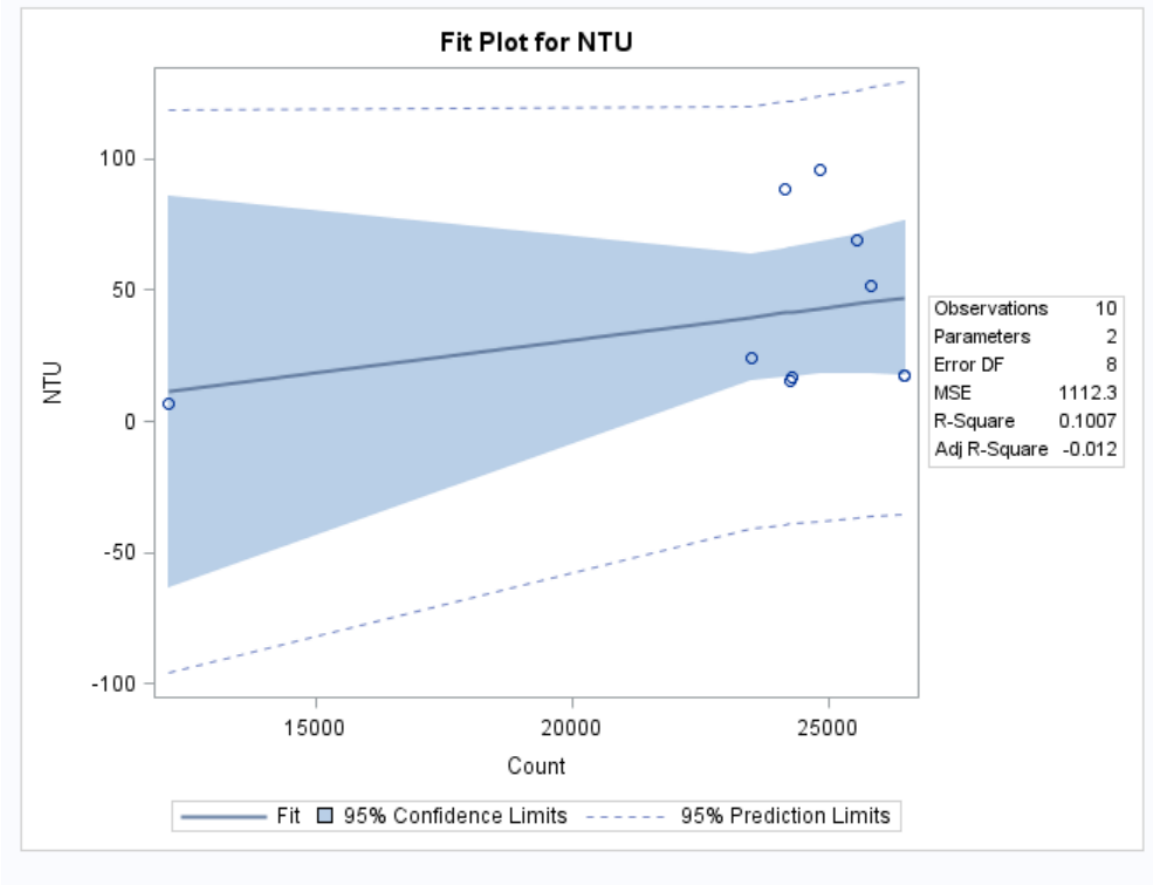


Figure D.4. shows the fit plot for count of particles vs NTU.

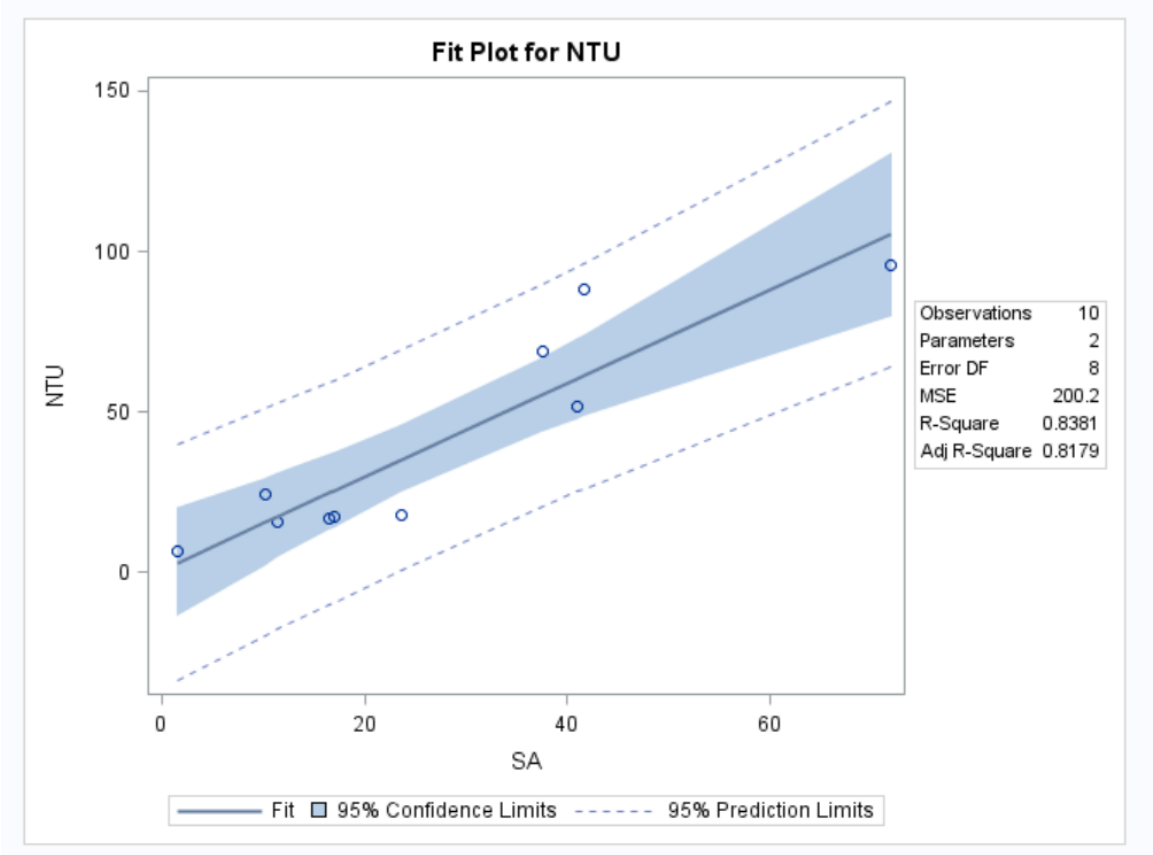


Figure D.5. shows the fit plot for surface area of particles vs NTU.

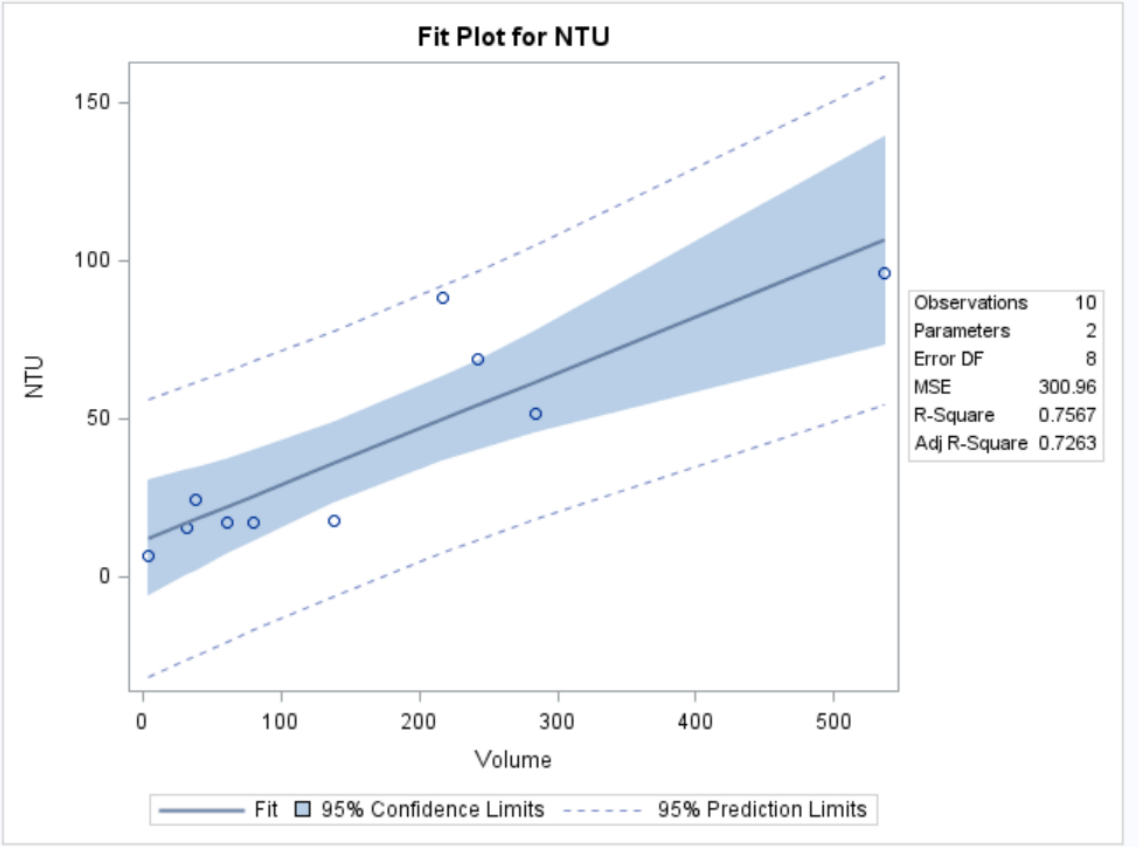


Figure D.6. shows the fit plot for volume of particles vs NTU.

# Appendix E. Media Types


Figure E.1. shows the Enhanced Nitrification media used in this study

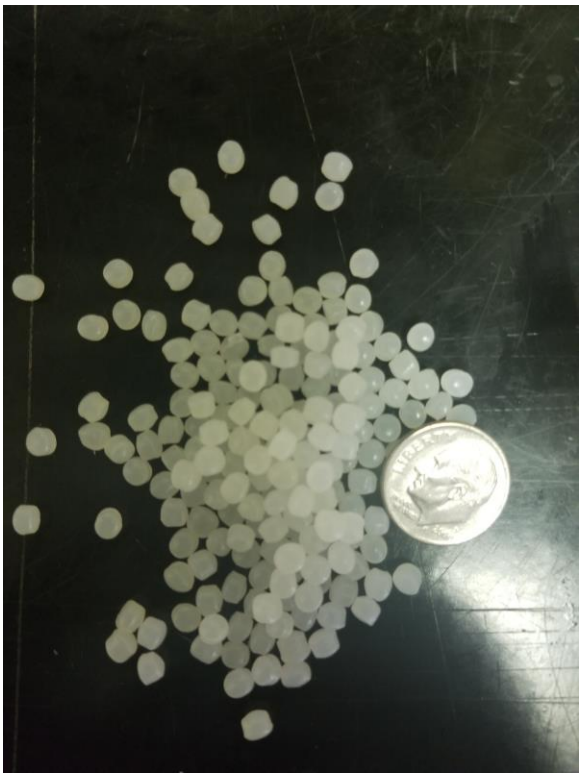

Figure E.2. shows the Standard media analyzed in this study

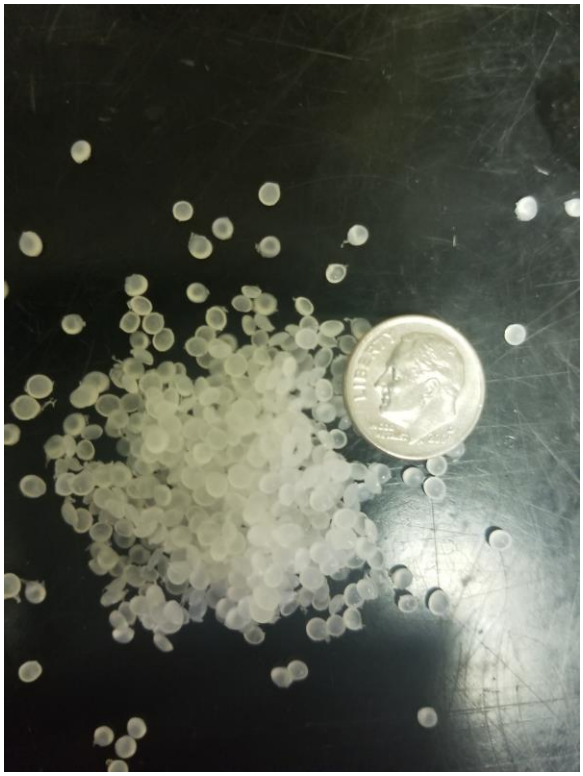

Figure E.3. shows the Fine Polyethylene Bead media used for this study

# VITA

Matthew Tyler Louque, born in Thibodaux, Louisiana, worked as an Engineering Student Intern for several years under his professor, Dr. Ronald Malone while pursuing his Bachelor's in Environmental Engineering from Louisiana State University. Upon completion of his degree, he continued working for his professor and went on to become certified as an Engineering Intern in the state of Louisiana. He then went on to reenroll at LSU to pursue a Master's degree in Civil and Environmental Engineering under advisement from Dr. Ronald Malone.